Chapter 14
A New Long-Necked Turtle, *Laganemys tenerensis* (Pleurodira: Araripemydidae), from the Elrhaz Formation (Aptian–Albian) of Niger

Paul C. Sereno and Sara J. ElShafie

Abstract An articulated skull and postcranial skeleton of a pelomedusoid turtle, *Laganemys tenerensis* gen. et sp. nov., is described from the Lower Cretaceous (Aptian–Albian) Elrhaz Formation in Niger. *Laganemys* has a proportionately long skull, which increases in depth anteriorly, from the occiput to the snout. The thin flat carapace and plastron are covered with fine sulcus-and-ridge texture. The carapace has a deep nuchal embayment anteriorly, a small mesoplastron laterally, and three median fenestrae. The cervical series is nearly as long as the carapace with specialized joints to enhance lateral flexion between cervicals 2 and 3 and cervicals 6 and 7. The relatively long tail is composed of at least 26 vertebrae. Forelimbs and hind limbs have long and relatively straight unguals. Discovered in a fluvial setting, *Laganemys* would have been an adept long-necked aquatic predator in still waters. A suite of derived features unites *Laganemys tenerensis* with *Araripemys barretoi*, a pelomedusoid from northeastern Brazil of similar form, habits and geologic age. These genera provide additional evidence of faunal exchange between South America and Africa in the mid Cretaceous (ca. 110 Mya) prior to the advent of deep waters in the central Atlantic Ocean.

Keywords *Araripemys* • Aquatic predation • Pelomedusidae • Pelomedusoides • Pleurodira

P. C. Sereno (✉) · S. J. ElShafie
Department of Organismal Biology and Anatomy, University of Chicago, 1027 East 57th Street, Chicago, IL 60637, USA
e-mail: dinosaur@uchicago.edu

S. J. ElShafie
e-mail: selshafie@uchicago.edu

Introduction

Pleurodires are less speciose than cryptodires among living turtles and are restricted in geographic range to freshwater habitats in the southern hemisphere. Pleurodiran diversity, habitats, and geographic range, however, were considerably greater in the past and appear to have peaked from the Late Cretaceous (ca. 100 Mya) through the Paleocene (ca. 55 Mya) (Gaffney et al. 2006). Preceding this rich record of pleurodiran diversity, however, is the first half of pleurodiran history. About 200 million years ago, pleurodires and cryptodires diverged from a common casichelydian ancestor, and for the ensuing 100 Mya the pleurodire fossil record is comparatively thin (Gaffney et al. 2006). The most complete pleurodire predating the Late Cretaceous is *Araripemys barretoi*, a small, flat-bodied, thin-shelled freshwater turtle (Fig. 14.1) known from several skeletons from the Araripe Basin of northeastern Brazil (Price 1973; Maisey 1991; Meylan 1996). Mid Cretaceous in age (Aptian–Albian), *Araripemys barretoi* is a pivotal species within Pleurodira and slightly older (ca. 110 Mya) than most other pleurodires. Extant pleurodires are divided into Chelidae and Pelomedusoides, and phylogenetic analysis has placed *Araripemys* as the outgroup to other pelomedusoids (Meylan 1996; Gaffney et al. 2006). Initially described on the basis of a partial shell (Price 1973), *Araripemys* is now known from several acid-prepared specimens that have allowed for a fairly complete cranial and postcranial osteological description (Meylan and Gaffney 1991; Meylan 1996; Gaffney et al. 2006).

Thin shell pieces with low, textured ornamentation and lightly impressed scute grooves similar to those in *Araripemys* were discovered in the mid Cretaceous (Aptian–Albian) Elrhaz Formation in Niger. On these fragmentary remains, Broin (1980) erected a new genus and species, *Taquetochelys decorata*, and mentioned the possible existence of a second species that might be referable to *Araripemys*. More recently, Fuente and Broin (1997) tentatively referred to *Araripemys* the anterior portion of a carapace and a fragmentary costal

D. B. Brinkman et al. (eds.), *Morphology and Evolution of Turtles,* Vertebrate Paleobiology and Paleoanthropology,
DOI: 10.1007/978-94-007-4309-0_14,

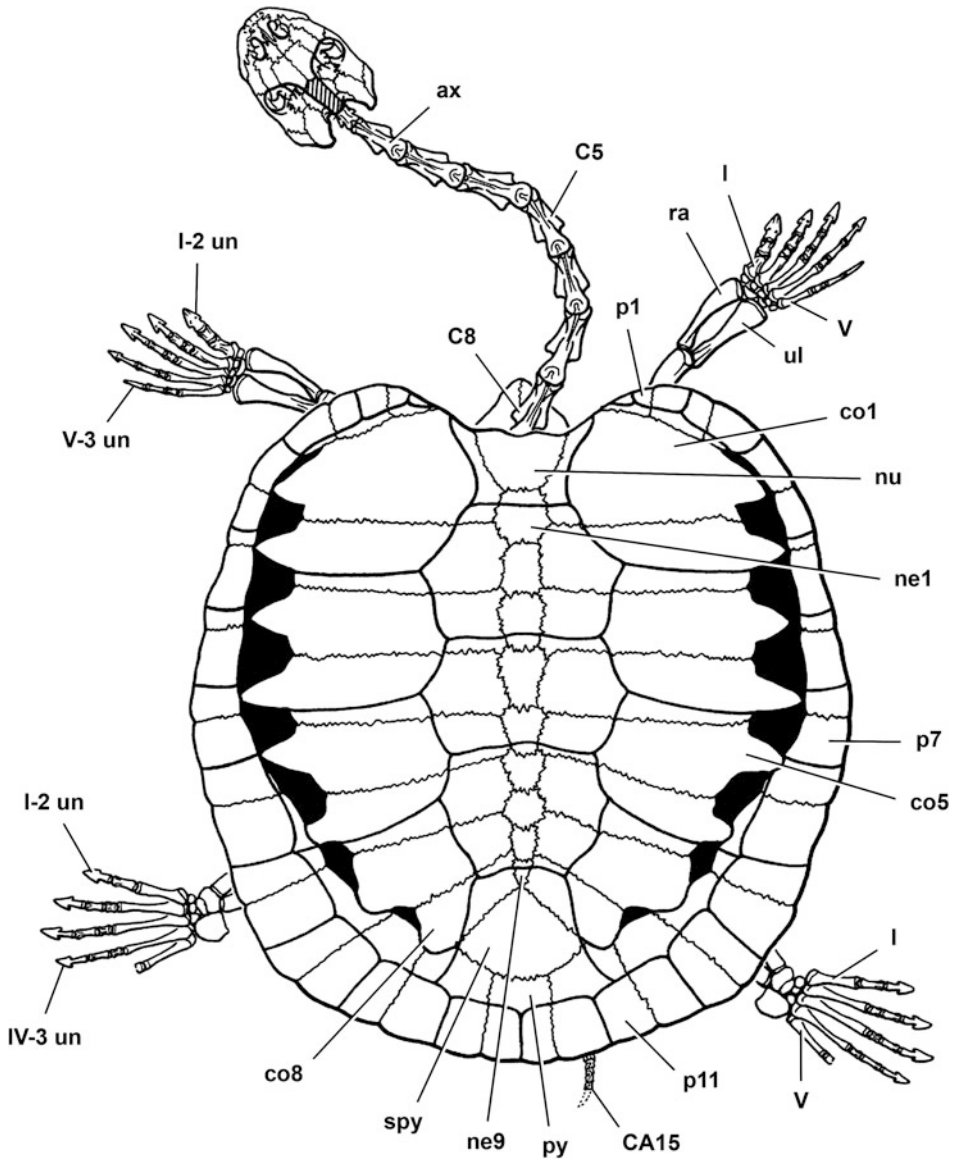

Fig. 14.1 Skeletal reconstruction of *Araripemys barretoi* Price 1973 in dorsal view (modified from Meylan and Gaffney 1991). Abbreviations: *I*, *IV*, *V* digits I, IV, V; *ax* axis; *C5*, *8* cervical vertebra *5*, *8*; *CA15* caudal vertebra *15*; *co1*, *5*, *8* costal *1*, *5*, *8*; *ne1*, *9* neural *1*, *9*; *nu* nuchal; *p1*, *7*, *11* peripheral *1*, *7*, *11*; *py* pygal; *ra* radius; *spy* suprapygal; *ul* ulna; *un* ungual

with similar pitted ornamentation from Paleocene deposits in northwestern Argentina. To date, these are the only reports on *Araripemys*-like turtles from outside the Araripe Basin since *A. barretoi* was described.

In 2000 a nearly complete turtle skeleton was recovered in the Elrhaz Formation (Aptian–Albian) of Niger (Sereno and ElShafie 2009). It was found 15–20 cm below the mid section of a skeleton of the large spinosaurid dinosaur, *Suchomimus tenerensis* (Sereno et al. 1998). At the time of its discovery, a portion of the left side of the shell and possibly the left hind limb broke away and disintegrated. The cross-section of the shell was exposed on the trench wall under the dinosaur skeleton, and the turtle and central portion of the dinosaur skeleton were collected in the same field jacket.

Preparation of the specimen revealed a remarkably complete articulated skeleton, including a skull and bones rarely preserved intact, such as the hyoids, carpus, manus and pes (Figs. 14.2, 14.3b, 14.4, 14.5, 14.6, 14.7, 14.8, 14.9, 14.10, 14.11, 14.12, 14.13, 14.14a, 14.15, 14.16, 14.17, 14.18, 14.20, 14.21, 14.22, 14.23). We describe this specimen below as the holotype of *Laganemys tenerensis* gen. et sp. nov, the first reasonably complete remains of a basal pelomedusoid discovered since description of *Araripemys barretoi* by Price in 1973.

The Elrhaz Formation is composed almost exclusively of medium-grained fluvial sandstone and is known for exquisite preservation of vertebrate material. Even by this preservational standard, the new thin-shelled turtle is exceptional. The much larger dinosaur immediately above the turtle is well preserved but only partially articulated; some of its bones

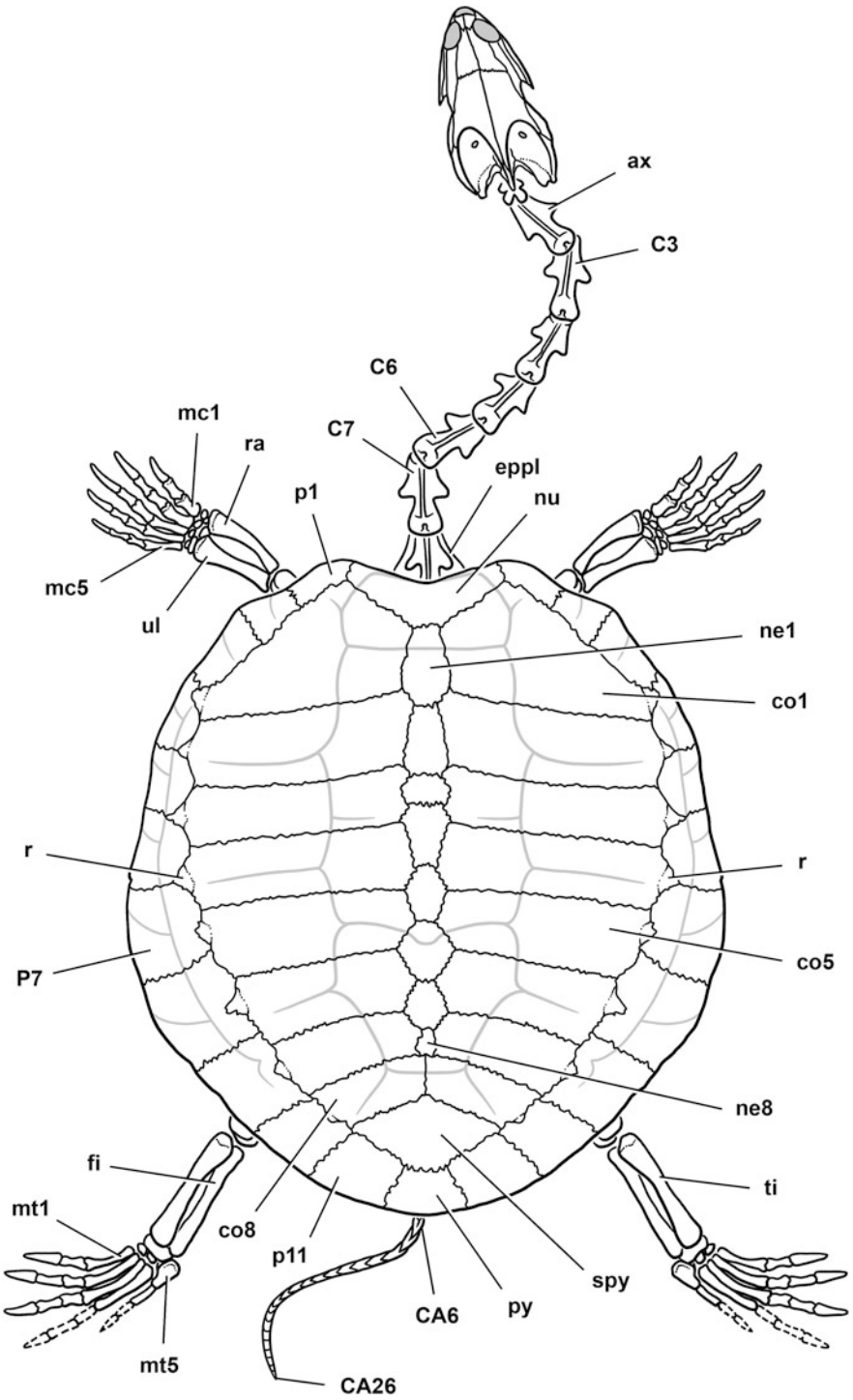

Fig. 14.2 Skeletal reconstruction of *Laganemys tenerensis* gen. et sp. nov. in dorsal view based on the holotypic skeleton (MNN GAD28). Visible scute margins indicated. Abbreviations: *ax* axis; *C3*, *6*, *7* cervical vertebra 3, 6, 7; *CA6*, *26* caudal vertebra 6, 26; *co1*, *5*, *8* costal 1, 5, 8; *eppl* epiplastron; *fi* fibula; *mc1*, *5* metacarpal 1, 5; *mt1*, *5* metatarsal 1, 5; *ne1*, *8* neural 1, 8; *nu* nuchal; *p1*, *7*, *11* peripheral 1, 7, 11; *py* pygal; *r* rib; *ra* radius; *spy* suprapygal; *ti* tibia; *ul* ulna

were transported postmortem. The turtle, on the other hand, is preserved with a high degree of natural articulation, including the skull, hyoids, cervical series, fore- and hind-limbs. It must have been buried quickly with only minor displacement, perhaps during transport and final burial of the overlying dinosaur skeleton.

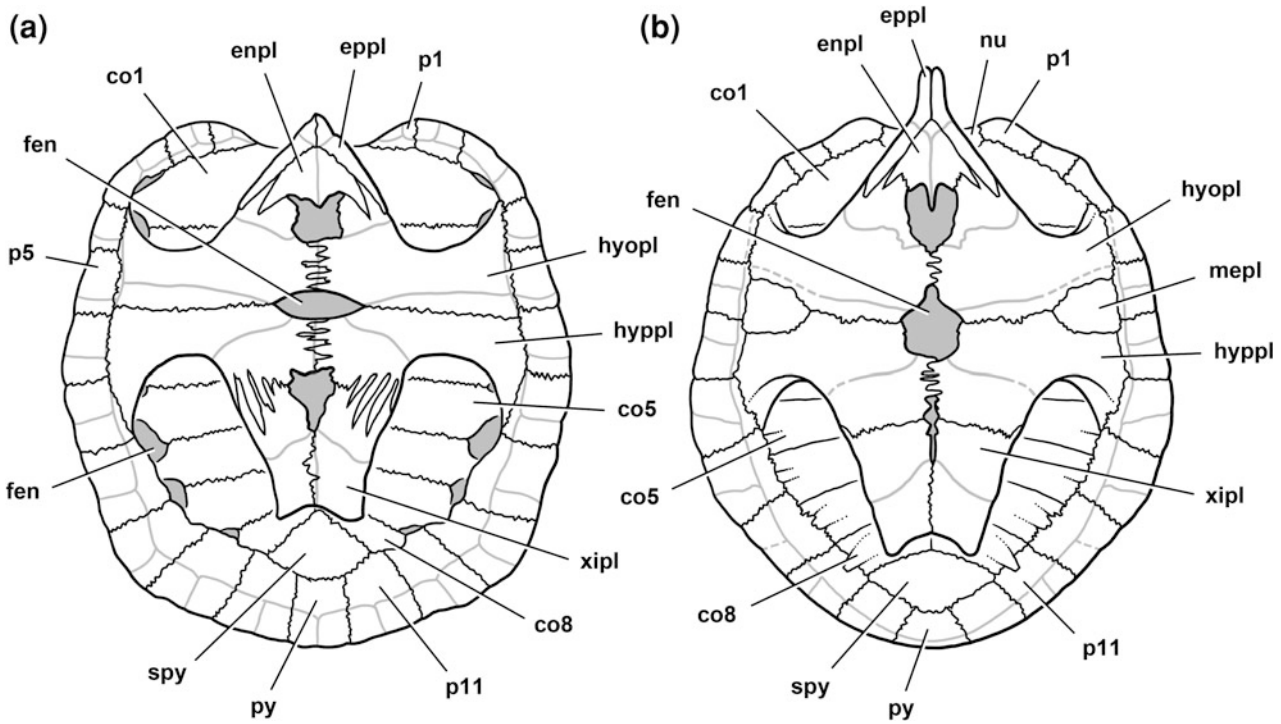

Fig. 14.3 Shell reconstruction in ventral view of *Araripemys barretoi* Price 1973 and *Laganemys tenerensis* gen. et sp. nov. **a** *Araripemys barretoi* Price 1973 based on several specimens (modified from Meylan and Gaffney 1991). **b** *Laganemys tenerensis* based on the holotypic skeleton (MNN GAD28). Visible scute margins indicated. Abbreviations: *co1*, *5*, *8* costal 1, 5, 8; *enpl* entoplastron; *eppl* epiplastron; *fen* fenestra; *hyopl* hyoplastron; *hyppl* hypoplastron; *mepl* mesoplastron; *nu* nuchal; *p1*, *5*, *11* peripheral 1, 5, 11; *py* pygal; *spy* suprapygal; *xipl* xiphiplastron

The shell is only slightly compressed dorsoventrally, the ends of the acromial processes projecting through the anterior plastral fenestra and the margins of the carapace pulled away from the plastral bridge (Fig. 14.13). Portions of the carapace are slightly ajar; the nuchal and anteriormost peripherals on the right side are shifted anteriorly and the costals are slightly telescoped in mid and posterior sections of the carapace (Fig. 14.11). Right and left sides of the plastron is slightly spread in anterior and mid sections (Fig. 14.13). The delicate neck, skull and tail are preserved largely in articulation. Of the extremities, only a portion of the right forelimb appears to be missing; the left hind leg was lost during collection.

Discovery of *Laganemys* provides additional evidence linking contemporary South American and African faunas prior to the opening of the central Atlantic Ocean around 100 Mya (Maisey 1993; Sereno et al. 2004). The vertebrate fauna from the Santana Formation in the Araripe Basin of Brazil and from the Elrhaz Formation in the Illumeden Basin of Niger are regarded as roughly comparable in age (Aptian–Albian, ca. 110 Mya). Their depositional settings, however, differ, the former predominantly lacustrine and the latter strictly fluvial. The remains of fish and thin-shelled turtles like *Araripemys*, as a result, are much more common in Araripe sediments than in the fluvial sandstones from Niger. The extraordinary preservation of the turtle we describe here thus adds an important taxon to this faunal comparison.

Institutional abbreviations used in this paper are: AMNH, American Museum of Natural History, New York, USA; MNHN, Musée National d'Histoire Naturelle, Paris, France; MNN, Museum National du Niger, Niamey, République du Niger; and UCRC, University of Chicago Research Collection, Chicago, Illinois, USA.

Systematic Paleontology

Testudines Linnaeus 1758
Pleurodira Cope 1865
Pelomedusoides de Broin 1988
Family Araripemydidae Price 1973 (= Araripemyidae Broin 1980)

Type genus and species: *Araripemys barretoi* Price 1973 (Figs. 14.1, 14.3a).

Distribution: Mid Cretaceous (Aptian–Albian) rocks in the Araripe Basin (Santana Formation) of Brazil and Illumeden Basin (Elrhaz Formation) of Niger.

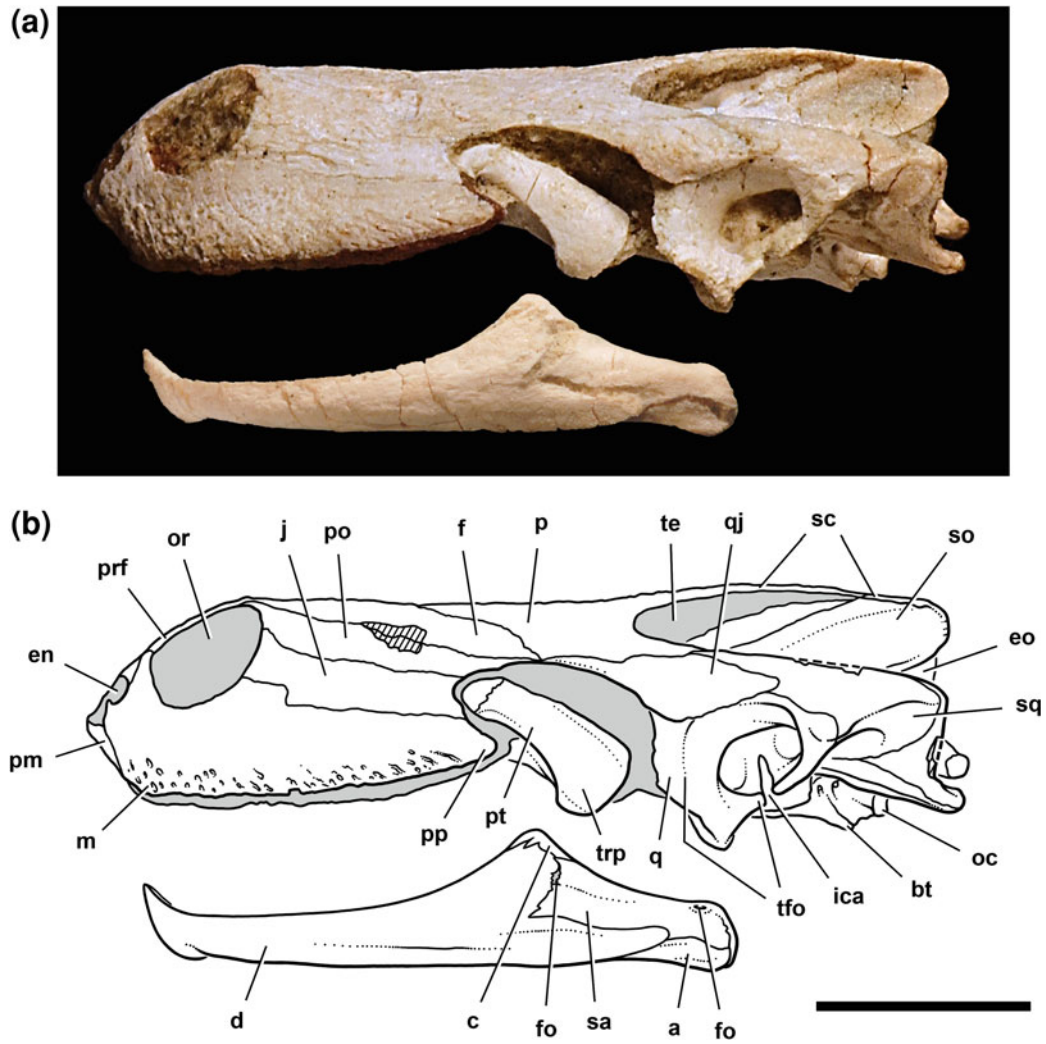

Fig. 14.4 Skull of *Laganemys tenerensis* gen. et sp. nov. (MNN GAD28) in left lateral view (reversed). **a** Photograph. **b** Line drawing. Scale bar = 1 cm. Abbreviations: *a* angular; *bt* basal tuber; *c* coronoid; *d* dentary; *en* external naris; *eo* exoccipital; *f* frontal; *fo* foramen; *ica* incisure of the columella auris; *j* jugal; *m* maxilla; *oc* occipital condyle; *or* orbit; *p* parietal; *pm* premaxilla; *po* postorbital; *pp* posterior process; *prf* prefrontal; *pt* pterygoid; *q* quadrate; *qj* quadratojugal; *sa* surangular; *sc* supraoccipital crest; *so* supraoccipital; *sq* squamosal; *te* temporal emargination; *tfo* tympanic fossa; *trp* trochlear process

Diagnosis: Basal pleurodires of modest body size (adult carapace length 10–30 cm) characterized by an elongate basisphenoid (50% of cranial length in the midline); carapace very thin (approximately 1 mm) with very low profile; fine-grained pit and ridge-and-sulcus texture on the external surface of the carapace, ventral aspect of the peripherals, and the external surface of the plastron; broad nuchal embayment; neural 3 with only four sutural contacts (neurals 2, 4; right and left costal 3); rib tips exposed on carapace with their distal tips projecting between adjacent peripherals (costals 1–4) or toward the central body of a single peripheral (costals 5–8); epiplastron strap-shaped; three median plastral fenestrae; scute margins lightly incised or absent on the carapace and plastron; cervical series (C1–8) elongate (90% of the length of the carapace); mid cervical transverse processes broad-based and subtriangular; postatlantal postzygapophyses partially or completely joined in the midline; cervical epipophyses wedge-shaped with a transverse distal margin and positioned adjacent to one another near the midline; and metacarpal 2 with a flange-like lateral buttress for metacarpal 3 along the proximal two-thirds of the shaft.

Remarks: Unable to refer *Araripemys* to any existing family, Price (1973) erected a monotypic Family Araripemydidae, which at that time was redundant with the genus and therefore carried no particular phylogenetic information. Subsequently, de Broin (1980) referred a second genus *Taquetochelys* to the Araripemydidae, although neither she nor later authors who described similar shell fragments from Argentina (Fuente and de Broin 1997) provided a familial diagnosis. Meylan (1996) also listed the family without diagnosis, referring to it an unnamed taxon from the Santana fauna (Gaffney and Meylan 1991). Fielding et al. (2005) erected a second species, *Araripemys arturi*, based on fragmentary and

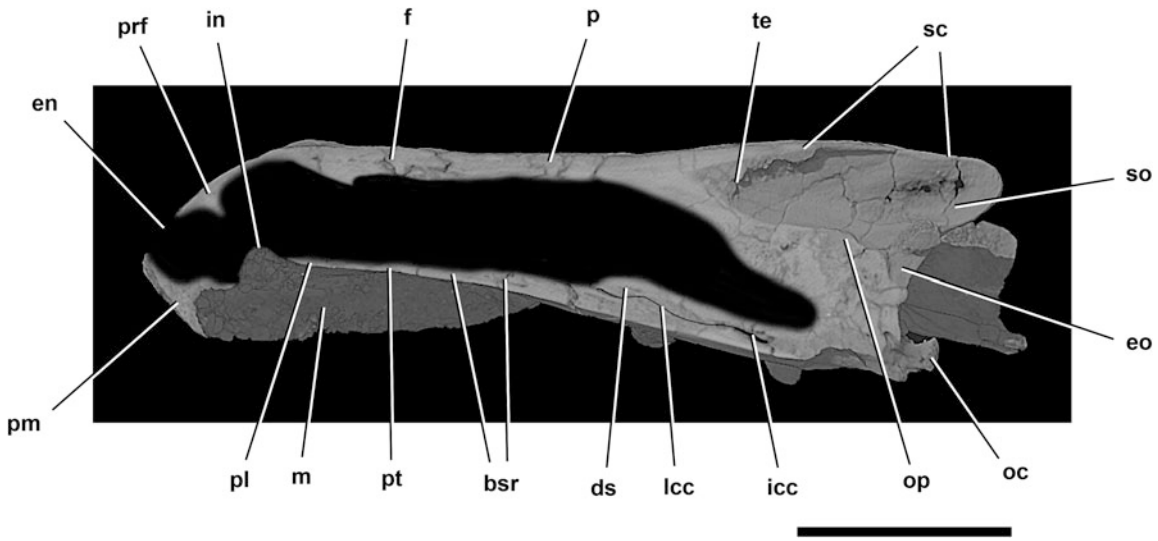

Fig. 14.5 Computed-tomographic reconstruction of the cranium of *Laganemys tenerensis* gen. et sp. nov. (MNN GAD28) in parasagittal cutaway view. Cross section is to the *left* of the midline in left lateral view. Scale bar = 1 cm. Abbreviations: *bsr* basisphenoid rostrum; *ds* dorsum sellae; *en* external naris; *eo* exoccipital; *f* frontal; *icc* internal carotid canal; *in* internal naris; *lcc* lateral carotid canal; *m* maxilla; *oc* occipital condyle; *op* opisthotic; *p* parietal; *pl* palatine; *pm* premaxilla; *prf* prefrontal; *pt* pterygoid; *sc* supraoccipital crest; *so* supraoccipital; *te* temporal emargination

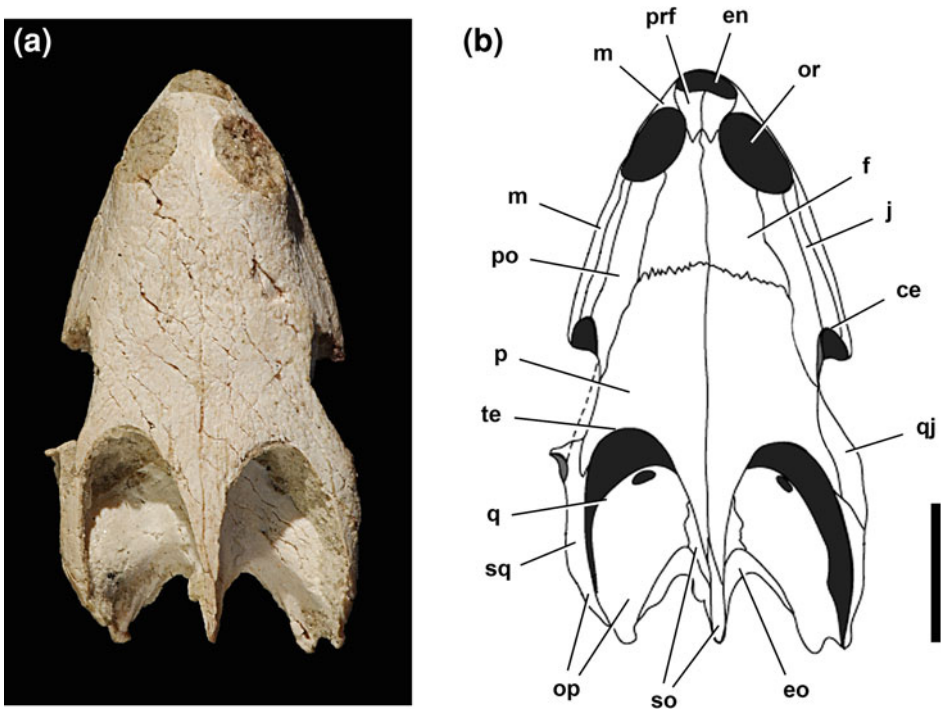

Fig. 14.6 Cranium of *Laganemys tenerensis* gen. et sp. nov. (MNN GAD28) in dorsal view. **a** Photograph. **b** Line drawing. Scale bar = 1 cm. Abbreviations: *ce* cheek emargination; *en* external naris; *eo* exoccipital; *f* frontal; *j* jugal; *m* maxilla; *op* opisthotic; *or* orbit; *p* parietal; *po* postorbital; *prf* prefrontal; *q* quadrate; *qj* quadratojugal; *so* supraoccipital; *sq* squamosal; *te* temporal emargination

immature material. Subsequent review regarded this poorly established taxon as a *nomen dubium* (Gaffney et al. 2006). As far as we are aware, we are the first to diagnose Araripemydidae as a nonredundant taxon. At present it contains the type genus *Araripemys* from Brazil and a second genus from Niger described below. We include only derived characters shared by both genera in the diagnosis given above.

Broin (1980) introduced "Araripemyidae," a variant spelling of the familial name Araripemydidae (Gaffney et al. 2006). Although Broin's variant is one of two spelling options recognized by the Code of Zoological Nomenclature for generating a familial name based on a genus, it was not the option chosen by the original author (Price 1973).

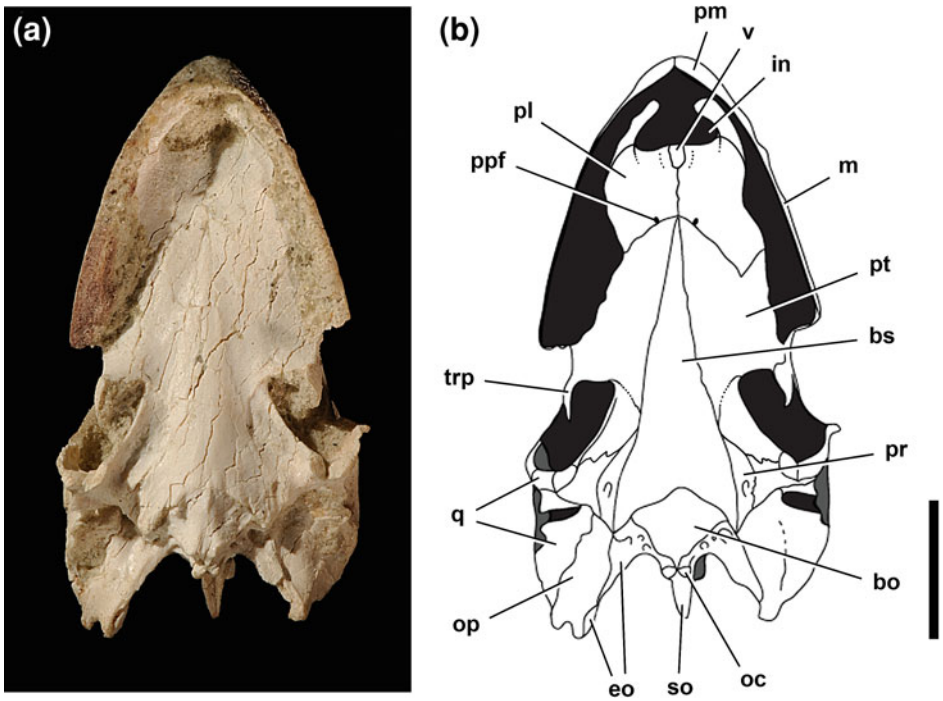

Fig. 14.7 Cranium of *Laganemys tenerensis* gen. et sp. nov. (MNN GAD28) in ventral view. **a** Photograph. **b** Line drawing. Scale bar = 1 cm. Abbreviations: *bo* basioccipital; *bs* basisphenoid; *eo* exoccipital; *in* internal naris; *m* maxilla; *oc* occipital condyle; *op* opisthotic; *pl* palatine; *pm* premaxilla; *ppf* posterior palatine foramen; *pr* prootic; *pt* pterygoid; *q* quadrate; *so* supraoccipital; *trp* trochlear process; *v* vomer

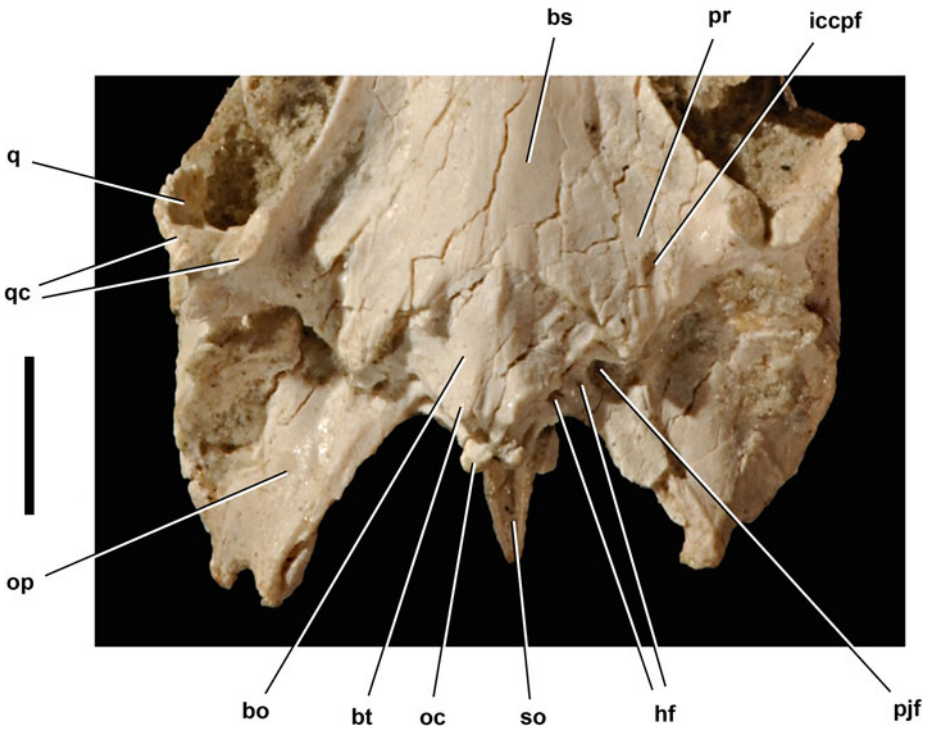

Fig. 14.8 Basicranium of *Laganemys tenerensis* gen. et sp. nov. (MNN GAD28) in ventral view. Scale bar = 5 mm. Abbreviations: *bo* basioccipital; *bs* basisphenoid; *bt* basal tuber; *hf* hypoglossal foramina; *iccpf* internal carotid canal, posterior foramen; *oc* occipital condyle; *op* opisthotic; *pjf* posterior jugular foramen; *pr* prootic; *q* quadrate; *qc* quadrate condyle; *so* supraoccipital

Araripemys Price 1973
Araripemys barretoi Price 1973
(Figs. 14.1, 14.3a).

Holotype locality, **unit**, **and age**: 2 kms northeast of Santana do Cariri, Ceará State, Brazil; Romualdo Member, Santana Formation, Araripe Basin; Aptian–Albian (Price 1973).

Revised diagnosis: Basal pleurodire of small size (adult carapace length 20–30 cm) with semicircular nuchal; costal 1 contributing to the anterior margin of the carapace (separating the nuchal and peripheral 1); peripheral 1 small, subtriangular; posterior margin of the carapace extended, with rectangular peripherals (long axis radial) that cover all but the distal shank, ankle and pes of an extended hind limb; mesoplastron

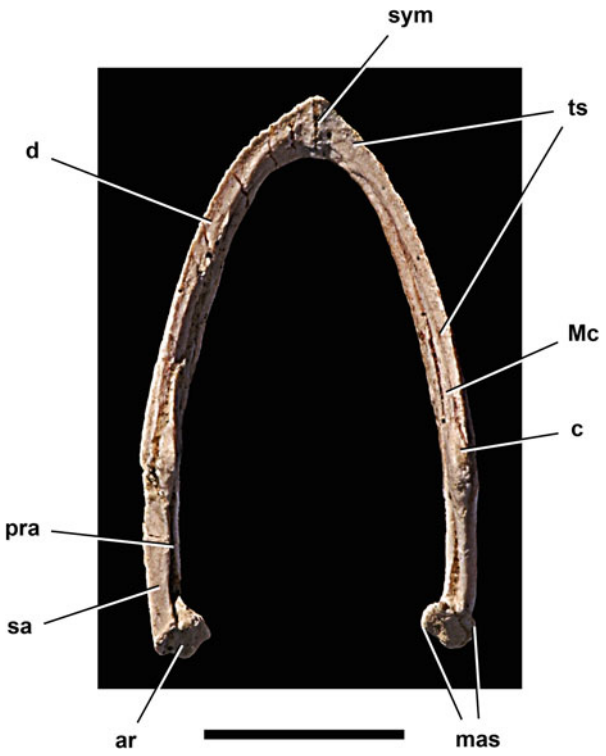

Fig. 14.9 Lower jaw of *Laganemys tenerensis* gen. et sp. nov. (MNN GAD28) in dorsal view. Scale bar = 1 cm. Abbreviations: *ar* articular; *c* coronoid; *d* dentary; *mas* mandibular articular surface; *Mc* Meckel's canal; *pra* prearticular; *sa* surangular; *sym* symphysis; *ts* triturating surface

Fig. 14.10 Ceratohyals of *Laganemys tenerensis* gen. et sp. nov. (MNN GAD28) in ventral view. Scale bar = 1 cm

absent; deeply interdigitating suture between the hypo- and xiphi-plastron; dorsal 1 firmly sutured to nuchal; arrowhead-shaped ungual phalanges on manus and pes.

Remarks: Meylan (1996, p. 20) and Gaffney et al. (2006, p. 35) provided diagnoses for this genus and species. The revised diagnosis restricts cited features to those that are, or could potentially be, autapomorphic.

Laganemys gen. nov.

Type species: *Laganemys tenerensis* sp. nov.

Etymology: *Lagano* (Greek), pancake; *emys* (Greek), turtle.

Diagnosis: Same as for type species.

Laganemys tenerensis sp. nov.
(Figs. 14.2, 14.3a, 14.4, 14.5, 14.6, 14.7, 14.8, 14.9, 14.10, 14.11, 14.12, 14.13, 14.14a, 14.15, 14.16, 14.17, 14.18, 14.20, 14.21, 14.22, 14.23).

Holotype: MNN GAD28, a nearly complete articulated skull and postcranial skeleton lacking the left posterolateral corner of the carapace and plastron, a few anterior caudal vertebrae, the right forelimb distal to the humerus, and the left hind limb.

Holotype locality, **unit**, **and age**: 16° 26′ 16.3 N, 9° 7′ 3.6 E (field locality 94, 2000 Expedition to Niger), Gadoufaoua, approximately 125 kms east of Agadez, Niger Republic; GAD 5 level in the Elrhaz Formation, Illumeden Basin; Aptian–Albian (Taquet 1976). Discovered in close association with the spinosaurid *Suchomimus tenerensis* (Sereno et al. 1998).

Etymology: *Tenere*, from Ténéré Desert; *ensis* (Latin), from.

Diagnosis: Basal pleurodire of small size (adult carapace length approximately 15 cm), skull very elongate (length more than five times maximum width) with snout increasing in depth anteriorly; maxilla with long posterior process ventral to the cheek emargination; postorbital excluded from the temporal emargination by quadratojugal-parietal contact; parietal-squamosal contact along the temporal emargination; parietal with posterolateral process; dentary ramus gently arched ventrally with squared distal end (chin) in lateral view; nuchal V-shaped; neural 3 small and rectangular with long axis oriented transversely, neural 8 small and rectangular (long axis sagittal), and neural 9 absent; epiplastron J-shaped; mesoplastron present and pentagonal; main forelimb bones (radius, metacarpal 2–4) considerably shorter (45–60%) than comparable hind limb bones (tibia, metatarsal 2–4); and metacarpal 2 with medially divergent distal condyles.

Remarks: de Broin (1980) erected a new taxon, *Taquetochelys decorata*, from the Elrhaz Formation (Aptian–Albian) of Niger. The material consists of 10 shell fragments (MNHN GDF838-848). The right hypoplastron (MNHN GDF847; Fig. 14.14b) was selected as the holotype (de Broin 1980, pl. III, Fig. 10); the other shell fragments were designated as paratypes (de Broin 1980, pl. III, Figs. 2–9, 11a, 11b).

The hypoplastron and other shell fragments were collected in isolation in the late 1960s and early 1970s during French expeditions to an area in the Ténéré Desert known as

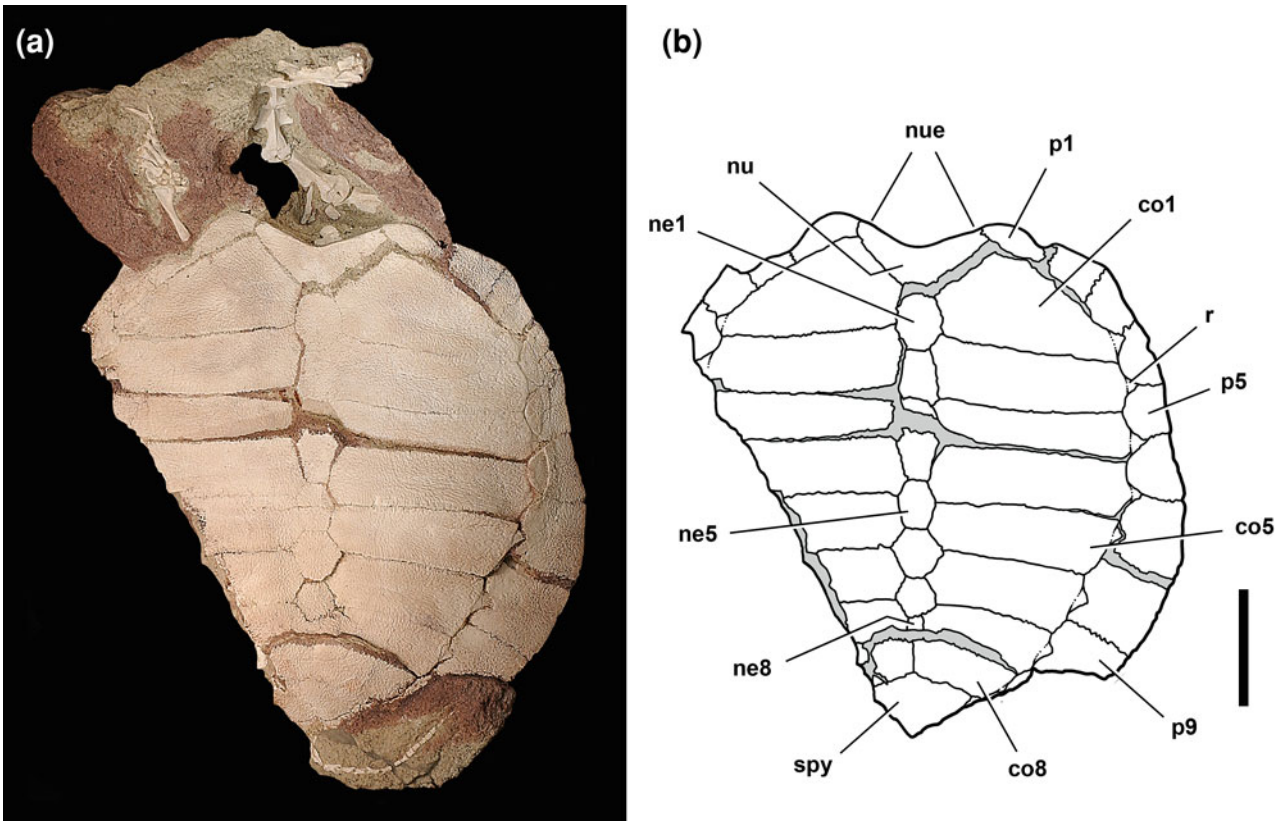

Fig. 14.11 Carapace of *Laganemys tenerensis* gen. et sp. nov. (MNN GAD28) in dorsal view. **a** Photograph. **b** Line drawing. Scale bar = 3 cm. Abbreviations: *co1*, *5*, *8* costal 1, 5, 8; *ne1*, *5*, *8* neural 1, 5, 8; *nu* nuchal; *nue* nuchal emargination; *p1*, *5*, *9* peripheral 1, 5, 9; *r* rib; *spy* suprapygal

Gadoufaoua (Taquet 1976). Unlike the other turtle remains described from Gadoufaoua by de Broin (1980), no locality information is given for the shell fragments referred to *T. decorata*, which may not pertain to a single individual given the abundance of disarticulated vertebrate remains in most exposures of the Elrhaz Formation. The new taxon, *Laganemys tenerensis*, was discovered at a new locality a number of kilometers away from previous localities (Taquet 1976, Figs. 7, 8). Nonetheless, as the holotype and only known specimen of was discovered in the same formation and region as the hypodigm of *T. decorata*, their taxonomic status as valid genera and species must be carefully considered.

Shape and textural differences are apparent between the holotypic hypoplastron of *T. decorata* and that in *L. tenerensis*, although both are thin, covered with a fine-grained ornamentation, and lie adjacent to a small mesoplastron (Fig. 14.14). Laterally the sutural margin for peripherals 5 and 6 in *L. tenerensis* is divided discretely into two parts, the suture for peripheral 6 angling posteromedially at approximately 30°; in *T. decorata* the margin is gently convex (Fig. 14.14). Anteriorly the sutural margin for the mesoplastron is different. In *L. tenerensis* the suture has a discrete angle of approximately 50°, giving the mesoplastron a distinctive pentagonal shape; in *T. decorata* this margin is more irregular (Fig. 14.14). The ramus of the hypoplastron between the mesoplastron and posterior embayment, as a result, is proportionately narrower in *L. tenerensis* than in *T. decorata*.

Posteriorly the margin of the embayment for the hind limb also shows differences. The contour of the embayment is more deeply arched in *L. tenerensis*, with a smooth margin approximately twice the width of that in *T. decorata* (Fig. 14.14). In *Araripemys barretoi*, the smooth margin is weakly developed or absent and the embayment has a broad contour as in *T. decorata*. The smooth margin, in addition, tapers to a point farther medially in *L. tenerensis*, medial to the apex of the embayment (Fig. 14.14).

A low texture is present across the surface of the plastron in both taxa, but it differs in the size and prominence of the pattern of dimples and pits and their organization into radiating ridges and sulci. We confine our comments to the hypoplastron, which de Broin (1980) designated as the holotype of *T. decorata*. The texture on the hypoplastron of *L. tenerensis* is dominated by ridge-and-sulcus texture, which covers most of the plate except for a transverse band in the posteromedial portion of the plate, where it merges into small subspherical pits less than 0.5 mm in diameter

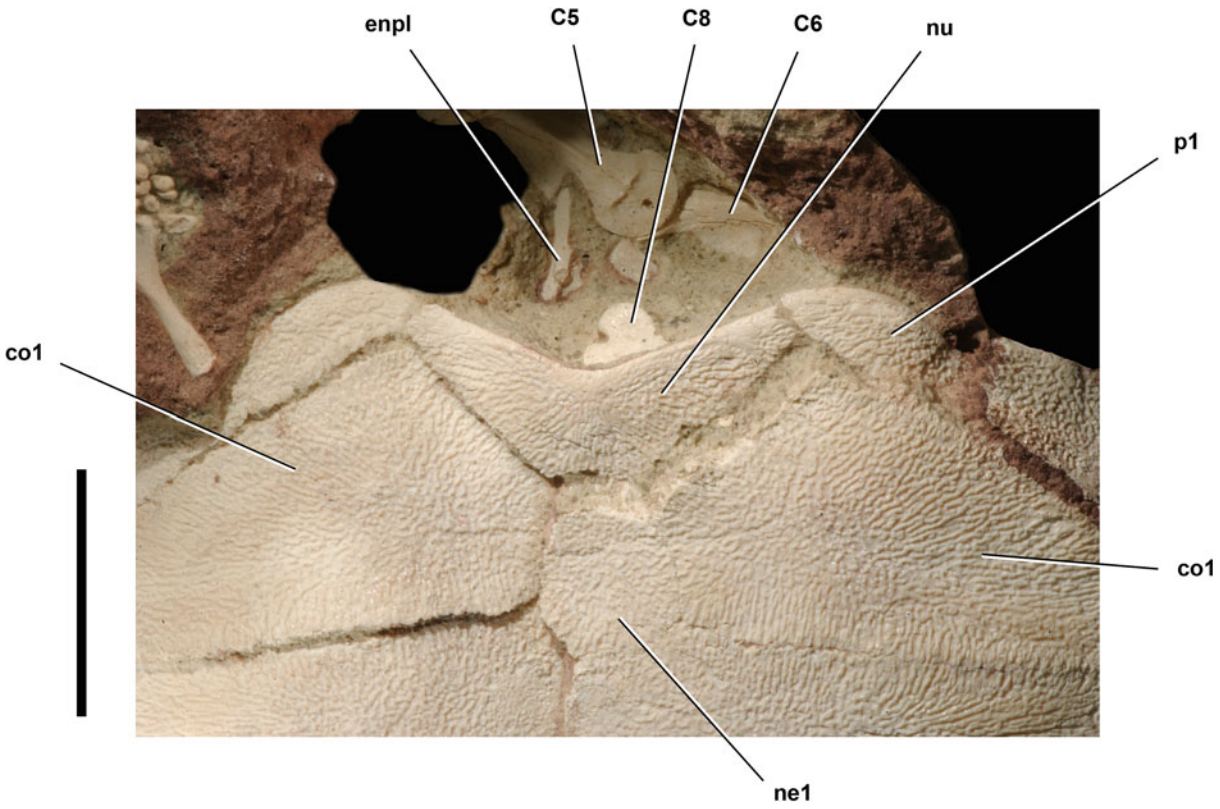

Fig. 14.12 Anterior portion of the carapace of *Laganemys tenerensis* gen. et sp. nov. (MNN GAD28) in dorsal view. Scale bar = 2 cm. Abbreviations: *C5*, *6*, *8* cervical vertebra 5, 6, 8; *co1* costal 1; *enpl* entoplastron; *ne1* neural 1; *nu* nuchal; *p1* peripheral 1

(Fig. 14.14a). The ridge-and-sulcus texture is organized into parallel ridges and grooves in the dorsal and posteromedial portions of the plate, and the ridges in general seem to emanate from what may constitute an ossification center near the apex of the embayment. In *T. decorata*, in contrast, the texture is dominated by subspherical dimples that merge into a ridge-and-sulcus texture only near the anterior and lateral margins of the hypoplastron (Fig. 14.14b). This dimpled texture, similar to the surface texture of a basketball, extends without diminution to the edge of the smooth inset margin of the posterior embayment. In *L. tenerensis*, in contrast, the ornamentation is noticeably reduced near the edge of the inset margin (Fig. 14.14a). Orientation of ridge-and-sulcus texture around a center is much less pronounced in *T. decorata*.

The shape and textural differences outlined above are noticeable and seem more substantial than variation attributable to age differences, individual variation, or sexual dimorphism. Although the material referred to *T. decorata* looks different than the holotype of *L. tenerensis*, we agree with Gaffney et al. (2006, p. 111) that the dimpled surface texture and other features of the holotypic hypoplastron of *T. decorata* are difficult to establish as autapomorphies justifying taxonomic distinction. Were the holotype closer in form to that of *L. tenerensis*, we may have been able to refer the new material to *T. decorata*, despite the very limited range of potentially diagnostic features in the holotypic hypoplastron. The range of differences does not allow that option. Furthermore, as additional araripemydids on Africa and elsewhere come to light, poorly established taxa such as *T. decorata* will only invite future taxonomic problems. We therefore regard the genus *Taquetochelys* and species *T. decorata* as *nomina dubia*.

Description

The skull and postcranial skeleton of *Laganemys* are well exposed and form the basis for this description. Computed-tomographic (CT) imaging of the cranium has revealed internal structure (Fig. 14.5). Future work on the cranium will include details of its neurovascular passages and endocranial volume. Future imaging of the postcrania will reveal structures currently obscured by matrix including the internal form of the shell, girdles and proximal limb bones.

We use "Romerian" rather than veterinarian terminology for orientation (e.g., "anterior" vs. "cranial") and refer to a trunk vertebra as a "dorsal" rather than a "thoracic"

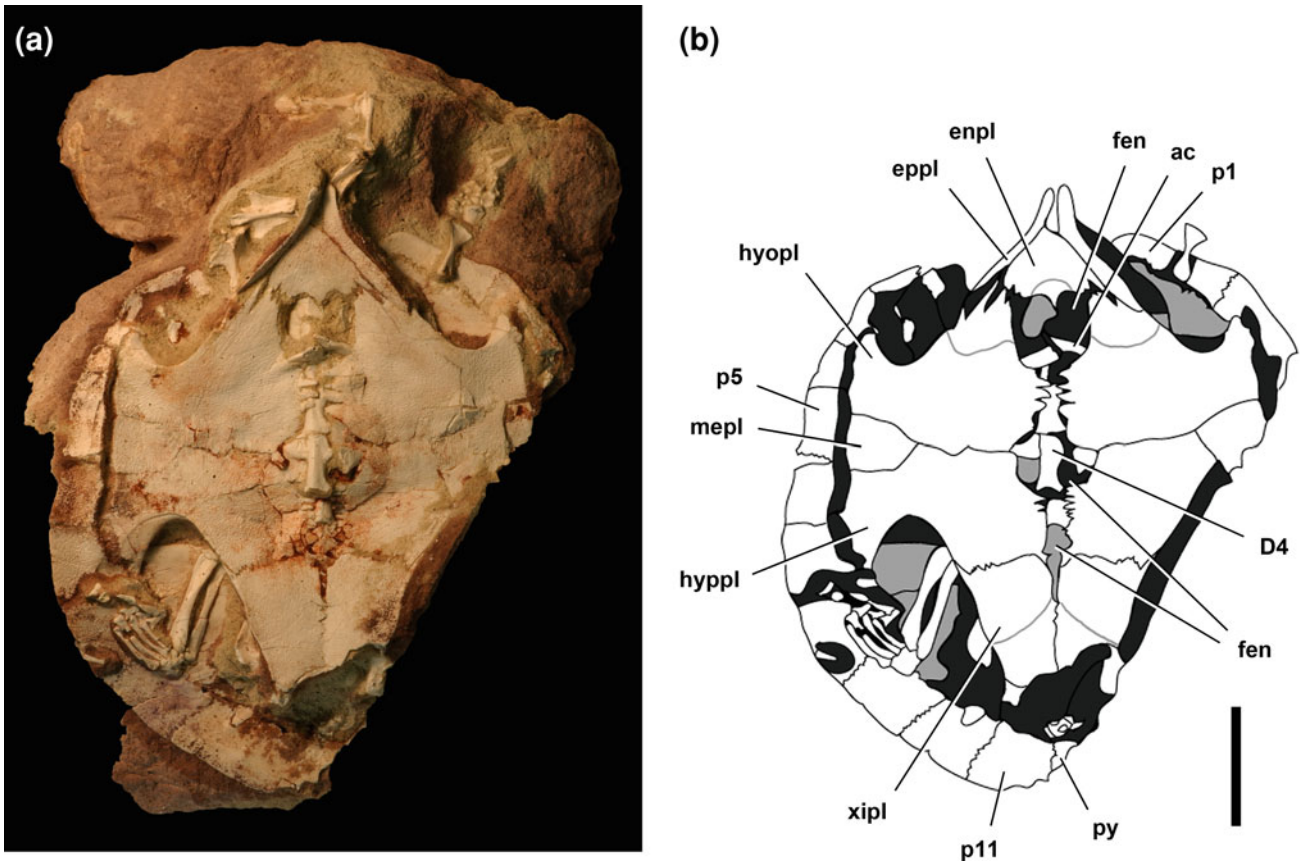

Fig. 14.13 Plastron of *Laganemys tenerensis* gen. et sp. nov. (MNN GAD28) in ventral view. **a** Photograph. **b** Line drawing. Scale bar = 3 cm. Abbreviations: *ac* acromion of the scapula; *D4* dorsal vertebra 4; *enpl* entoplastron; *eppl* epiplastron; *fen* fenestra; *hyopl* hyoplastron; *hyppl* hypoplastron; *mepl* mesoplastron; *p1*, *5*, *11* peripheral 1, 5, 11; *py* pygal; *xipl* xiphiplastron

(Romer 1956; Wilson 2006). In the skull, we follow the anatomical terminology summarized by Gaffney (1972) but express all terms in English. For the subset of specialized cranial structures sometimes expressed in Latin (Gaffney 1972), the Latin equivalents are given in parentheses on first usage. Neither standardized veterinarian terminology nor Latin have been shown to enhance accuracy in anatomical communication over Romerian equivalents (Wilson 2006).

Skull: The skull of *Laganemys* is proportionately longer than in *Araripemys*, due largely to the extension in the middle portion of the skull. In lateral view of the skull of *Laganemys* (Fig. 14.3), the orbit and cheek emargination are separated by a long sheet of bone. In *Araripemys*, in contrast, the posterior margin of the orbit and anterior margin of the cheek emargination are near one another (Meylan 1996). Likewise, in lateral view in *Laganemys* the cheek emargination is situated entirely anterior to the temporal emargination (Fig. 14.4), whereas in *Araripemys* they broadly overlap. As a result the trochlear process of the pterygoid (processus trochlearis pterygoidei) is situated anterior to the temporal fossa (fossa temporalis superior) in *Laganemys* (Fig. 14.4), whereas in *Araripemys* it is exposed in dorsal view of the skull through the temporal fossa (Meylan 1996).

The depth of the anterior end of the cranium in *Laganemys* is very distinctive as well. The cranium is deepest at the orbits (Fig. 14.2; Table 14.1) and increases approximately by 20% at its anterior end (Fig. 14.4); this is not the case in *Araripemys* (Meylan 1996). The cheek emargination is dorsoventrally deep in both *Laganemys* and *Araripemys*, but in the former the embayment extends farther anteriorly, resulting in a longer pointed posterior process on the maxilla (Fig. 14.4). The cheek emargination is also visible as an embayment along the lateral side of the skull in dorsal view (Fig. 14.6). The temporal emargination is proportionately narrower in *Laganemys* (Fig. 14.6), whereas in *Araripemys* the fossa is roughly as long as wide in dorsal view of the skull (Meylan 1996).

The subcircular orbits are slightly longer anteroposteriorly than deep and are directed laterally as much as dorsally as in *Araripemys* (Figs. 14.4, 14.6). The aspect of the orbits that sets *Laganemys* apart is the gentle telescoping, or eversion, of the posterior half of the orbital margin.

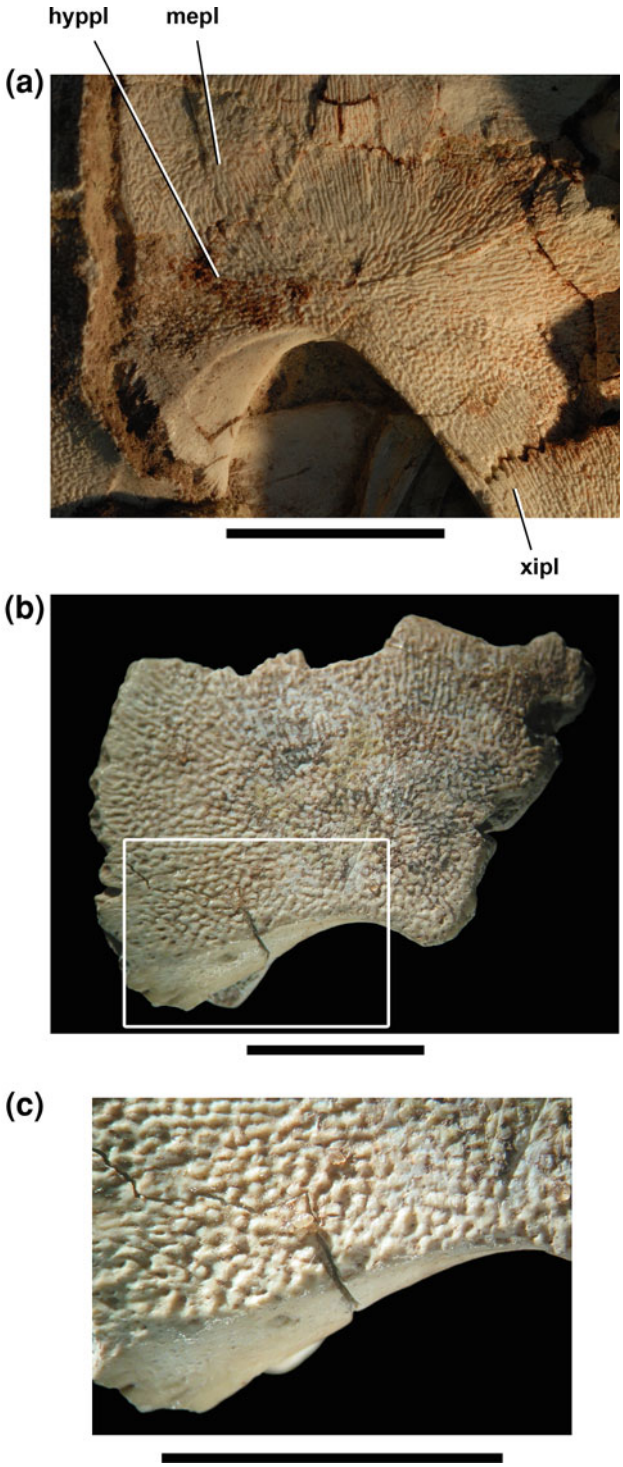

Fig. 14.14 Hypoplastron of *Laganemys tenerensis* gen. et sp. nov. (MNN GAD28) and *Taquetochelys decorata* (MNHN GDF847) in ventral view. **a** Right hypoplastron of *Laganemys tenerensis*. **b** Right hypoplastron of *Taquetochelys decorata*. **c** Magnified view of posterior margin of the right hypoplastron of *Taquetochelys decorata*. Scale bar = 2 cm in **a** and 1 cm in **b** and **c**. Abbreviations: *hyppl* hypoplastron; *mepl* mesoplastron; *xipl* xiphiplastron

The skull roof is composed of the usual set of paired roofing elements; nasals are absent as in other pelomedusoids (Meylan 1996; Gaffney et al. 2006). The supraoccipital crest (crista supraoccipitalis) extends as far posteriorly as the posterolateral process, the latter formed by the squamosal and opisthotic (Fig. 14.6). In both *Laganemys* and *Araripemys*, the supraoccipital crest and posterolateral processes extend far posterior to the occipital condyle.

In ventral view the labial ridge formed by the premaxilla and maxillae is narrower than in *Araripemys* (Fig. 14.7). The labial ridges of upper and lower jaws (Fig. 14.9), thus, are more V-shaped than U-shaped. The basisphenoid contribution to the palate equals or exceeds that of other palatal bones, none of which bear teeth. The ramus of the lower jaw (Figs. 14.4, 14.9) is considerably longer and more slender in *Laganemys* as compared to *Araripemys* (Meylan 1996; Gaffney et al. 2006).

Dorsal skull roof: The *premaxilla* is fused with its opposite medially and to the maxilla posteriorly, obliterating most of its external sutures. A portion of the premaxilla–maxilla suture appears to be preserved on the right side, marking the edge of a transversely narrow, deep bone in external view. Its palatal sutures and surface are recessed above and anterior to the labial ridge and are obscured by matrix (Figs. 14.5, 14.7). Exposed sutural contacts, thus, are limited to the maxilla. In anterior view the premaxillae join along the ventral margin of the external naris (apertura narium externa) and form a subtriangular dorsomedian process that partially divides the opening. The external surface of the bone is pitted. The labial ridge curves dorsally near the midline, forming with its opposite a V-shaped notch to receive the pointed anterior end of the mandible (Fig. 14.9). *Araripemys* does not appear to have a similar premaxillary notch (Meylan 1996).

The *maxilla* contacts the premaxilla and prefrontal anteriorly and the jugal posteriorly, forming the lateral margin of the external naris and the ventral margin of the orbit. The anterior end of the maxilla extends dorsally along the anterior margin of the orbit as a slightly raised, tapering prong. In *Araripemys*, the maxilla extends dorsally adjacent to the external naris, not the orbit (Meylan 1996). On the posterior side of the orbit, the maxilla-jugal suture steps ventrally before passing posteriorly (Fig. 14.4). The posterior position of the maxilla-jugal suture on the orbital margin in *Laganemys* differs from the ventral position of the suture in *Araripemys* (Meylan 1996). The maxilla forms most of the posterior process under the cheek emargination. The external surface is pitted above the labial ridge, with some of the pits forming shallow concavities under the orbit (Fig. 14.4). The posterior process is marked by low posteroventrally inclined ridges and some small foramina.

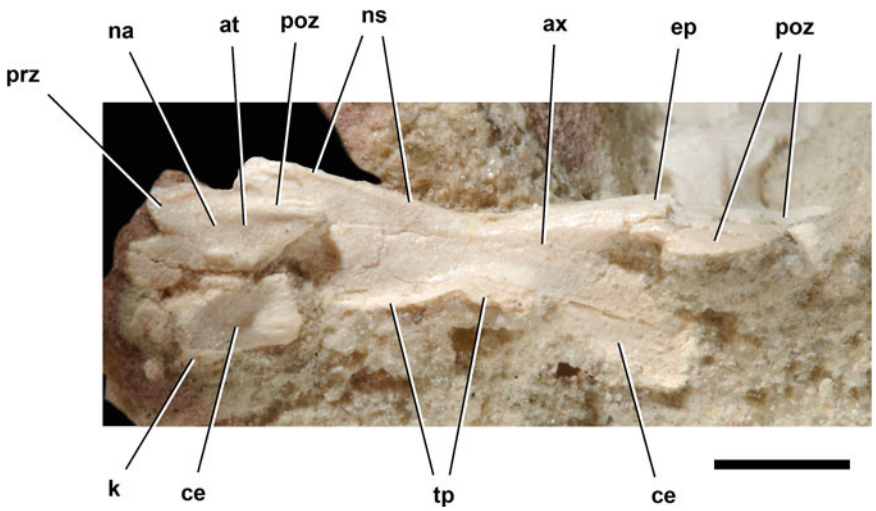

Fig. 14.15 Atlas and axis of *Laganemys tenerensis* gen. et sp. nov. (MNN GAD28) in left lateral view. Scale bar = 5 mm. Abbreviations: *at* atlas; *ax* axis; *ce* centrum; *ep* epipophysis; *k* keel; *na* neural arch; *ns* neural spine; *poz* postzygapophyses; *prz* prezygapophysis; *tp* transverse process

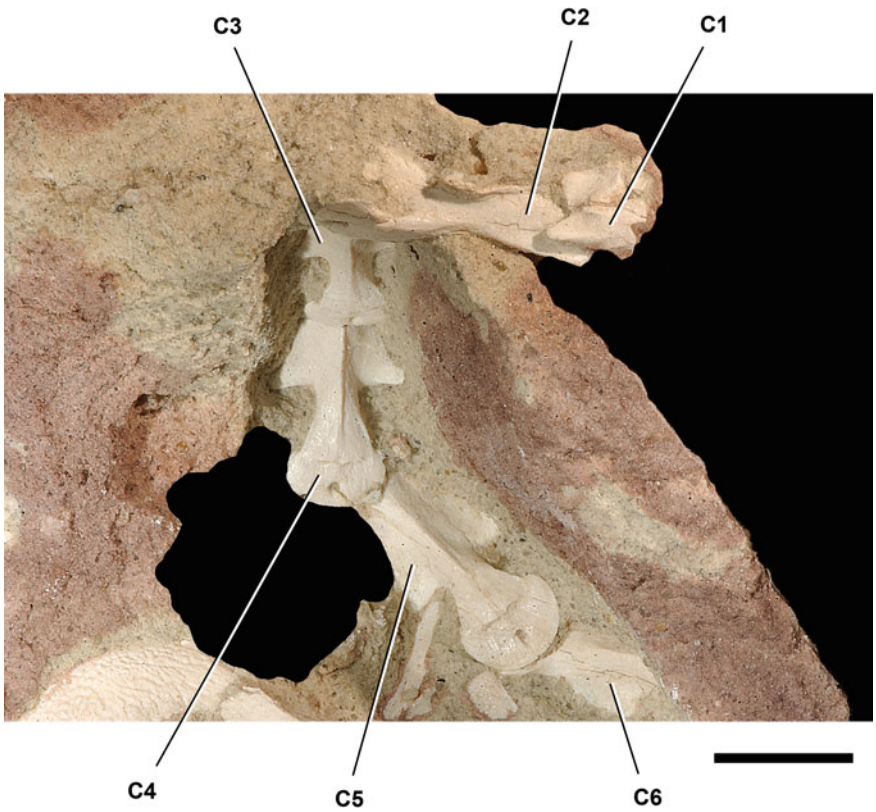

Fig. 14.16 Anterior and mid cervical vertebrae of *Laganemys tenerensis* gen. et sp. nov. (MNN GAD28) in lateral and dorsal view. Scale bar = 1 cm. Abbreviations: *C1–6* cervical vertebrae 1–6

In ventral view, a portion of the maxilla-palatine suture is exposed on the left side of the palate. The maxilla shares the triturating surface along its length with the palatine. In *Araripemys*, in contrast, the narrower triturating surface is limited to the maxilla (Meylan 1996). The internal nares together form a subtriangular opening with a broad, transverse posterior margin. The maxilla forms the lateral side of each internal naris and is separated from the footplate of the vomer by the palatine.

The *jugal* is a strap-shaped bone that extends from the posterior margin of the orbit to the deepest notch of the cheek emargination (Fig. 14.4). Its contacts include the postorbital dorsally, the maxilla ventrally and the quadratojugal posteriorly. Unlike *Araripemys*, the jugal margin of the orbit is distinctly everted. The jugal contacts the base of the trochlear process of the pterygoid but does extend onto the palate as in *Araripemys* (Meylan 1996; Gaffney et al. 2006).

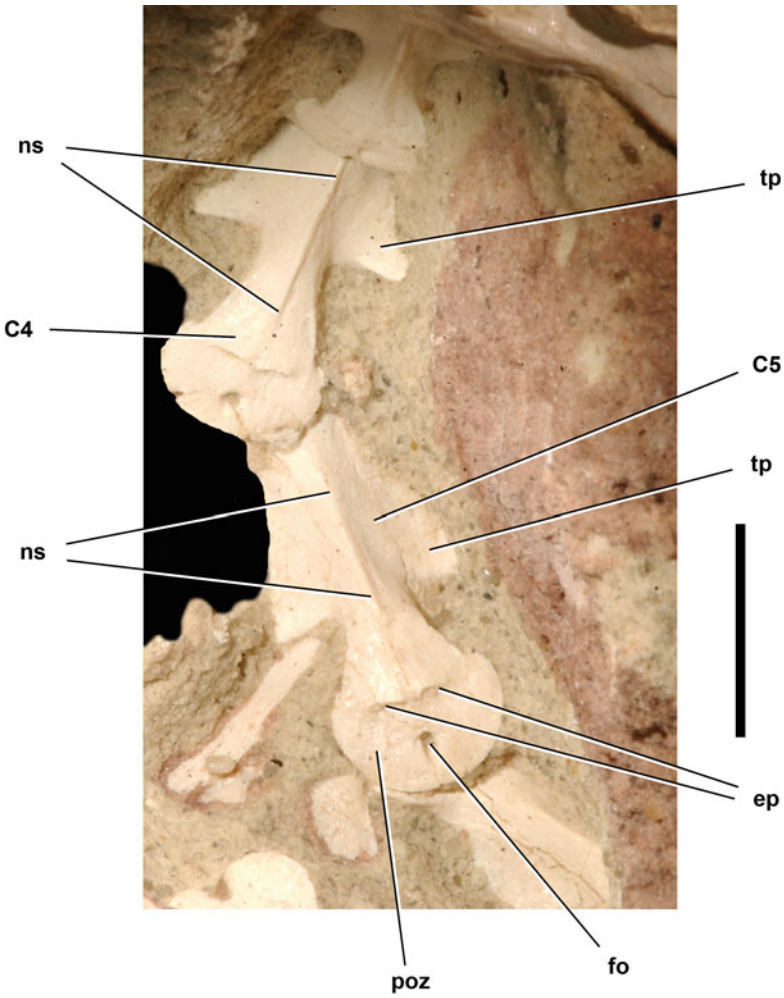

Fig. 14.17 Cervical vertebrae 4 and 5 of *Laganemys tenerensis* gen. et sp. nov. (MNN GAD28) in dorsal view. Scale bar = 1 cm. Abbreviations: *C4, 5* cervical vertebra 4, 5; *ep* epipophysis; *fo* foramen; *ns* neural spine; *poz* postzygapophyses; *tp* transverse process

The *postorbital*, like the jugal, is strap-shaped, extending from the orbit to the cheek emargination. The postorbital contacts the frontal and parietal dorsomedially and the jugal ventrally. The posterior tip of the postorbital contacts the anterior tip on the quadratojugal along the cheek emargination. The orbital margin formed by the postorbital is telescoped like that of the adjacent jugal. Unlike *Araripemys* and most pelomedusoids, the postorbital does not reach the superior temporal fossa (Fig. 14.6).

The *quadratojugal*, which is best preserved on the right side, is a diamond-shaped bone contacting the parietal dorsally and the squamosal and quadrate posteriorly. Ventrally the quadratojugal borders the posterior half of the cheek emargination. Dorsally it fails to separate the parietal and squamosal, which meet along the temporal emargination, an unusual sutural configuration among pleurodires.

The *squamosal* contacts the quadratojugal and a slender process of the parietal anteriorly and the quadrate ventrally and the exoccipital (Fig. 14.4). It forms the majority of the lateral rim of the temporal emargination and extends posteriorly along the posterolateral side of the skull. In this region it joins the opisthotic to form a prominent posteriorly projecting process, as in *Araripemys* and other pelomedusoids such as *Euraxemys* (Meylan 1996; Gaffney et al. 2006).

The *prefrontal*, a subtriangular plate that is thin in cross-section (Fig. 14.5), forms the posterior margin of the external naris and the anteromedial margin of the orbit (Fig. 14.6). The prefrontal is gently transversely arched along the narial opening, where it contacts the maxilla. It extends posterodorsally as a tapering plate, its distal tip overlapping the frontal and terminating in a V-shaped posterior suture. Comparatively, *Araripemys* has been shown with both a V-shaped (Meylan 1996) and interdigitating (Gaffney et al. 2006) prefrontal–frontal suture. The orbital margin of the prefrontal, which is not telescoped, is restricted to the anteromedial margin by an ascending process of the maxilla. This differs from the condition in *Araripemys*, where the prefrontal borders the ventral orbital margin (Meylan 1996; Gaffney et al. 2006). The contacts of the prefrontal within the orbit are visible only in the CT scan.

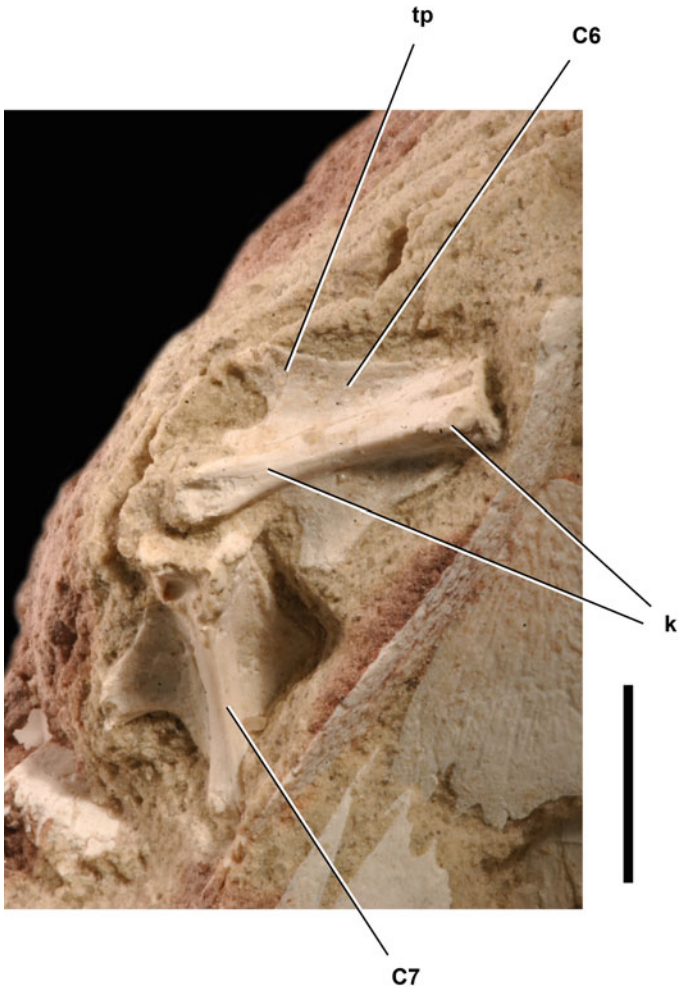

Fig. 14.18 Cervical vertebrae 6 and 7 of *Laganemys tenerensis* gen. et sp. nov. (MNN GAD28) in ventral view. Scale bar = 1 cm. Abbreviations: *C6*, *7* cervical vertebra 6, 7; *k* keel; *tp* transverse process

The *frontal* is overlapped anteriorly by the prefrontal, abutts laterally against the postorbital, and meets the parietal posteriorly along an interdigitating suture (Fig. 14.6). The frontoparietal suture is near the posterior margin of the orbit in *Araripemys*, whereas in *Laganemys* it is located approximately one-third of the distance along the dorsal skull roof between the orbit and temporal emargination. The orbital rim formed by the frontal is gently everted.

The *parietal* extends across the posterior two-thirds of the skull roof from its interdigitating contact with the frontal anteriorly to the sides of the supraoccipital on the supraoccipital crest posteriorly (Fig. 14.6). In parasagittal section, both the frontal and parietal are relatively thick (Fig. 14.5). The parietal meets the postorbital and quadratojugal laterally along a nearly straight suture, with its distal tip contacting the squamosal. The posterior margin of the parietal is deeply embayed by the temporal emargination, forming a distinctive posterolateral process. In *Araripemys* there is no parietal-quadratojugal or parietal-squamosal contact and no development of a posterolateral process (Meylan 1996; Gaffney et al. 2006).

Palate: The outer margin of the palate, including nearly the entire triturating surface for the mandible, is formed by the premaxilla and maxilla. The remainder of the palate is composed of the quadrate, pterygoid, palatine and vomer (Fig. 14.7) and slopes posteroventrally at approximately 15° from the internal naris (apertura narium interna) to the ventral surface of the occiput (Fig. 14.5).

The internal narial opening is at least partially divided posteriorly by the *vomer*, a bone that was not preserved in the acid-prepared crania of *Araripemys* (Meylan 1996; Gaffney et al. 2006). The vomer is absent in many extant pelomedusids (Gaffney 1979; Gaffney et al. 2006), but this does not appear to be the case among araripemydids. In *Laganemys* the posterior portion of the bone is preserved as a tongue-shaped median element, presumably the posterior ends of fused right and left vomers (Fig. 14.7). The footplate appears to overlap right and left palatines, although their contact is developed as an interdigitating suture.

The *palatine* forms the posterior margin of the internal naris, which is depressed centrally where the palatine and footplate of the vomer meet (Fig. 14.7). The palatine

Table 14.1 Measurements (mm) of the holotypic skeleton (MNN GAD28) of the mid Cretaceous pelomedusoid turtle *Laganemys tenerensis* gen. et sp. nov.

Measurement		Code
Cranium		
Length, premaxilla to distal tip of supraoccipital crest	40	I
Length, premaxilla to occipital condyle	37	A
Width, maxillary flange to opposite	20	B
Width, across quadrate condyles	20	–
Preorbital length	3	–
Postorbital length, orbital margin to tip of supraoccipital crest	31	–
Depth, orbital roof to maxillary labial ridge	10	–
Depth, parietal roof to maxillary labial ridge	8	–
Depth, supraoccipital crest to quadrate condyle	13	G
Depth, supraoccipital crest to occipital condyle	10	K
Orbit, anteroposterior diameter	6	D
Orbit, dorsoventral diameter	5	J
Interorbital width	3	C
External nares, width	4	E
Posterior palate, width between inferior temporal fossae	9	N
Internal nares, width	6	F
Premaxilla–maxilla labial ridge, length	21	–
Lower Jaws		
Midline length	28	A
Symphysis to coronoid process, length	20	B
Mid length, depth	3	–
Ramus at coronoid process, width	2	C
Hyoid Ossification		
Ceratohyal length	(26)	
Axial Skeleton		
Carapace, maximum length	144	
Carapace, midline length	137	
Carapace, maximum width	140	
Plastron, maximum length	130	
Plastron, maximum width	101	
Plastral bridge, minimum anteroposterior length	38	
Cervical 1, intercentrum length	5	
Cervical 2, centrum length (without odontoid)	16	
Cervical 4, centrum length	17	
Cervical 6, centrum length	17	
Cervical 7, centrum length	17	
Dorsal 2, centrum length	15	
Dorsal 3, centrum length	13	
Dorsal 4, centrum length	13	
Caudal 4, centrum length	5	
Caudal 6, centrum length	4	
Caudal 12, centrum length	2	
Caudal 19, centrum length	2	
Caudal 21, centrum length	1	

(continued)

Table 14.1 (continued)

Measurement	Code
Appendicular Skeleton	
Radius length	16
Ulna length	16
Metacarpal 1 length	(5)
Metacarpal 2 length	6
Metacarpal 4 length	8
Metacarpal 5 length	7
Manual digit I, phalanx 1 length	4
Manual digit II, phalanx 2 length	3
Manual digit II, ungual length	6
Manual digit III, phalanx 2 length	4
Manual digit III, ungual length	7
Manual digit IV, phalanx 1 length	3
Manual digit IV, phalanx 2 length	4
Manual digit IV, ungual length	6
Manual digit V, ungual length	4
Tibia length	27
Metatarsal 1 length	13
Metatarsal 2 length	15
Metatarsal 3 length	17
Metatarsal 4 length	15
Pedal digit I, phalanx 1 length	5
Pedal digit I, ungual length	7
Pedal digit II, phalanx 1 length	4
Pedal digit II, ungual length	6
Pedal digit III, phalanx 1 length	4
Pedal digit III, ungual length	5

Measurements of paired structures are from the right side, except those from the forelimb. In right column, letter code after cranial measurements corresponds to measurement diagrams for the cranium and lower jaws in Gaffney et al. (2006, Appendices 4, 8); in same column, symbol "–" indicates no corresponding letter code

descends laterally to meet the maxilla along the margin of the palate. At their junction, the palatine sends a prong-shaped process anteriorly over the maxilla along the lateral side of the internal naris. The palatine is overlapped by a very short triangular process of the maxilla, before the suture turns posteriorly along the triturating surface. In *Araripemys* the palatine does not contribute to the triturating surface, which is composed solely of the maxilla (Meylan 1996; Gaffney et al. 2006). In *Laganemys* the medial one-half of the triturating surface is formed by the palatine, a subtle lingual ridge apparent on the palatine indicating the medial margin of the keratinous sheath.

The palatines meet along an interdigitating median suture, which extends posteriorly to meet the apex of the basisphenoid and the anteromedial corners of the pterygoids at a single point (Fig. 14.7). A posterior palatine foramen (foramen palatinum posterius) is located to each side of the midline within the palatine near the palatine-pterygoid suture. The left foramen is positioned slightly more anteriorly than the right foramen, which lies on the anterior side of the interdigitating palatine-pterygoid suture. This foramen is larger and situated farther laterally on the palate in *Araripemys* (Meylan 1996; Gaffney et al. 2006). The palatine extends posteriorly in the mid palate, forming a V-shaped suture with the pterygoid before reaching the lateral side of the palate. Contact in this region with the jugal is obscured by matrix.

The *pterygoid* contacts the palatine anteriorly along a suture, most of which is interdigitated. The long medial suture with the basisphenoid appears to be fused (Fig. 14.7). Other contacts near the basisphenoid include the prootic and quadrate. Lateral contact with the jugal is partially exposed at the base of the trochlear process within the cheek emargination (Fig. 14.4). The trochlear process angles

posteroventrally from the jugal-pterygoid suture, extending posteroventrally as a hatchet-shaped, pendant flange below the cheek emargination. The lateral surface is lightly textured and separated from the palatal surface by a distinct edge. The expanded distal end of the trochlear process is dorsoventrally convex.

A crescentic, flange of the pterygoid is elevated slightly from the palatal surface, lying between the basisphenoid and inferior temporal fossa (Fig. 14.7). The arcuate medial margin of this flange extends from the edge of the trochlear process and curves along the lateral margin of the basisphenoid and prootic, and then forms an interdigitating suture with the quadrate near the mandibular condyles (condylus mandibularis). This crescentic palatal surface is more clearly demarcated than in other pleurodires, with the medial edge invaginated into the basisphenoid.

The *quadrate* in lateral view forms the smooth curved wall of the tympanic fossa (cavum tympani) and contacts in this region the quadratojugal and squamosal (Fig. 14.2). In ventral view, quadrate forms the mandibular condyles and extends medially to contacts the prootic and opisthotic. A fissure, the incisure columella auris, is present on the ventral wall of the tympanic fossa. The fossa extends posteromedially into the braincase as the postotic antrum, an internal space hidden in lateral view by the posterior rim of the tympanic fossa.

The relatively flat mandibular condyles are deeply cleft, with the medial condyle facing ventrolaterally at approximately 45° to the sagittal plane (Figs. 14.7, 14.8). The lateral condyle is flat and faces anteroventrally at approximately 45° to a transverse plane. The condition is similar to that in *Araripemys* (Meylan 1996; Gaffney et al. 2006). Contact with the pterygoid is initiated just above the condyles and extends medially until reaching the prootic.

Braincase: The *prootic* contacts the quadrate laterally, the opisthotic posteriorly, and a small margin of the supraoccipital posteromedially and the basisphenoid medially (Figs. 14.6, 14.7, 14.8). The prootic, exposed as a crescent between the quadrate and basisphenoid in ventral view, is marked by the posterior opening of the internal carotid artery (foramen posterior canalis carotici interni), the principal arterial supply to the brain. Although the prootic is fused to adjacent elements, the fused sutures are still discernible.

In dorsal view, the *opisthotic* contacts the supraoccipital medially, the prootic anteriorly, and the quadrate laterally. The opisthotic forms the core of a prominent paroccipital process (processus paroccipitalis) that extends posteriorly as far as the supraoccipital crest (Figs. 14.5, 14.6). In ventral view, the opisthotic is bordered laterally by the quadrate and medially by the exoccipital.

The *supraoccipital* forms the narrow apex of the relatively large, teardrop-shaped foramen magnum. The supraoccipital extends from this point on the foramen magnum posteriorly, forming the base and posterior tip of the supraoccipital crest. In sagittal view, the supraoccipital crest does not extend posteriorly as far as the paroccipital process and posterior extremity of the squamosal (Fig. 14.5). The very thin central portion of the crest thickens toward its ventral margin, which is concave and confluent with the dorsal border of the foramen magnum.

The *exoccipitals* form the prominent, thin sidewalls of the foramen magnum, joining the supraoccipital dorsally and the basioccipital ventrally. Between these contacts, the exoccipital extends posterolaterally along the proximal one-half of the paroccipital process. Gaffney et al. (2006) describe a small foramen opening on the exoccipital-opisthotic suture on the paroccipital process. This foramen is not present in *Laganemys*. In the body of the bone, however, are three foramina, a large posterior jugular foramen (foramen jugulare posterius) and two smaller foramina for the hypoglossal nerve (foramina nervi hypoglossi; Fig. 14.8). The exoccipital contacts the basisphenoid just anterior to these foramina. The exoccipital extends posteriorly to form a rounded occipital condyle (condylus occipitalis) that is crescentic in posterior view. Between opposing crescentic condyles, lies a central fossa. As in Pelomedusidae, the occipital condyles are composed exclusively of the exoccipitals. In *Araripemys*, in contrast, the basisphenoid forms a small median ventral condyle. The differing structure of the occipital condyles between *Laganemys* and *Araripemys* is one of the few features which would link one of these genera with another pelomedusoid and thus is indicative of homoplasy.

The *basioccipital* is exposed ventrally as a transversely broad and convex, diamond-shaped bone. Anteriorly near its contact with the basisphenoid, there is a shallow median keel. The keel dissipates posteriorly, with a pair of low wedge-shaped basal tubera (tuberculum basioccipitale) developed in conjunction with the exoccipitals. The basioccipital has a small triangular median process extending between the tubera, but it stops short of the occipital condyles (Fig. 14.8). In *Araripemys*, in contrast, the basioccipital has been shown to contribute the ventral one-third of the occipital condyle (Gaffney et al. 2006). This portion of the skull is well preserved and highlights a significant structural difference.

The *basisphenoid* forms a long, narrow-shaped ramus that extends along the midline for over half the skull length in ventral view, dividing the pterygoids to each side and establishing a point contact with the palatines (Fig. 14.7). The basisphenoid is relatively long in *Laganemys* and *Araripemys* compared to other pleurodires.

Lower jaw: A complete mandible was present and consists of six articulated bones, the dentary, coronoid, surangular, angular, prearticular, and articular (Figs. 14.4b,

14.9). The splenial is not present, a condition common to all pelomedusoids. The conjoined lower jaws have the form of a slightly bowed, pointed arch in dorsal or ventral view (Fig. 14.9). The articular surface for the quadrate condyles (area articularis mandibularis) is set slightly medial to the lateralmost arc of the dentary ramus. The dentary ramus is proportionately long to match the proportionately long cranium. The coronoid region, for example, is positioned in the posterior 25% of the lower jaw, and the depth of the dentary ramus at mid length is only 3 mm (Table 14.1). The lower jaw differs from that of *Araripemys* by its much longer proportions and ventral curvature, pointed anterior end, and absence or reduction of internal and external foramina.

The *dentary* ramus is slender with a very thin triturating edge forming its dorsal margin. In lateral view the axis of the ramus curves ventrally toward the symphysis, its anterior end squared and slightly expanded to form a "chin" ventrally and a pointed apex dorsally. The dorsal apex fits into a notch in the upper jaws between the premaxillae. A suture separates the dentaries at the symphysis as in *Araripemys* and some pelomedusids (Meylan 1996). As in *Araripemys*, the dentary extends far posteriorly, terminating in a pair of tongue-shaped processes, one at the root of the coronoid rise and a second longer one lateral to the adductor fossa (Fig. 14.4b). Sutural contacts of the dentary include the coronoid, surangular and angular. In medial view, the triturating surface is well developed along the entire upper margin of the dentary and is broadest at mid length, angling approximately 45° ventromedially. Anteriorly and posteriorly, the triturating surface narrows in width and is more strongly inclined. Meckel's groove (sulcus cartilaginis meckelii) first appears near the symphysis and deepens posteriorly.

A subtriangular *coronoid* is exposed laterally and, to a greater extent, medially. It forms the top of the coronoid rise and encloses Meckel's canal medially. The posterior margin of the coronoid joins the prearticular on the anterior rim of the adductor fossa. Sutural contacts of the coronoid include the dentary, surangular and prearticular.

The *surangular* is best exposed in lateral view, where it contacts the dentary, coronoid, angular and articular. The auriculotemporal foramen (foramen nervi auriculotemporalis), if correctly identified as such, is very small and located near the dorsal margin of the surangular (Fig. 14.4b, fo). In most basal pelomedusoids and *Araripemys* (Meylan 1996), in contrast, the auriculotemporal foramen is considerably larger and located on the lateral aspect of the surangular, serving as an exit from the adductor fossa for a branch of the chorda tympani nerve (Gaffney 1972, Fig. 17). *Foxemys* and all later pelomedusoids, however, lack this foramen (Gaffney et al. 2006), and so there remains some doubt regarding the identity of the small, dorsally positioned foramen in *Laganemys*. At the base of the coronoid process, a horizontal groove leads anteriorly to the sutural triple-junction between the surangular, dentary and coronoid (Fig. 14.4b). A gap at this sutural junction may have served as another opening in the sidewall of the mandible in *Laganemys*.

The *angular* is a strap-shaped bone best exposed in medial view along the ventral margin of the jaw. The angular tapers to a slender process anteriorly at mid length along the dentary ramus, enclosing Meckel's canal (fossa meckelii) posteriorly and tapering to a point along the ventral margin of Meckel's groove anteriorly. Posteriorly the angular maintains its width as it extends under the articular at the jaw articulation. Sutural contacts include the dentary, surangular, prearticular and articular. Along the angular–prearticular suture on both sides, a small internal mandibular foramen (foramen intermandibularis caudalis) is visible.

The *prearticular* is another strap-shaped postdentary bone exposed only in medial view of the lower jaw. Its contacts include the dentary, angular, coronoid and articular. The prearticular forms the medial wall of the adductor fossa and extends to the end of the lower jaw under the articular.

The *articular* is a small wedge-shaped bone that contacts the angular, surangular and prearticular (Fig. 14.9). The angular and surangular overlap the articular laterally and remain as a distinctive flange at the end of the lower jaw, separated from the articular by a suture filled with matrix. This angular–surangular flange appears to contact the lateral quadrate condyle. The articular, which is positioned medial to this flange, has an articular surface that is angled posteroventrally at approximately 45° from the horizontal, as seen in medial or lateral view of the lower jaw. The articular surface is ovate, a little deeper than broad and divided into two transversely concave facets by a rounded median keel. The keel articulates with the groove between the flat quadrate condyles. Below the articular surface, the posterior foramen for the chorda tympani nerve (foramen posterius chorda tympani) enters the articular to access the adductor chamber (Gaffney 1972).

Hyoid: A pair of curved, rod-shaped bones is preserved in association ventral to the cervical series (Fig. 14.10). We identify these as ceratohyals (= cornua), which in turtles and other reptiles are often curved, rod-shaped bones that broaden and flatten slightly toward their proximal articular ends (Romer 1956). The distal end of the ceratohyal is rod-shaped and more slender than the flattened proximal end, the articular head of which appears to have broken away.

The ceratohyal measures 23 mm in length and may have been 26 mm long as a complete element, or approximately 65% of skull length (Table 14.1). The ceratohyal in *Araripemys* has a more robust shaft and is proportionately

shorter, measuring approximately 50% of skull length (Gaffney et al. 2006, Fig. 31B).

Shell ornamentation: A radiating ridge-and-sulcus texture is present on most of the external surfaces of the carapace and plastron. Each ridge or sulcus is spaced approximately 0.5 mm apart and typically radiates from a central locus on each plate (Figs. 14.11, 14.12, 14.13a, 14.21). The ridge-and-sulcus texture also occurs on the ventral surface of the peripherals. On some of the peripherals, the texture is limited to the outer margin; adjacent to the bridge of the plastron, the texture covers the entire ventral surface (Figs. 14.14a, 14.23). The ventral surface of costal and neural plates on the interior aspect of the shell is smooth. The ridge-and-sulcus texture, thus, is present on surfaces with external exposure, and a similar texture is present on the external surfaces of the skull. In *Araripemys* the external texture on the shell is pitted to a greater degree, although we regard fine-grained pit and ridge-and-sulcus texture as a synapomorphy of the Araripemydidae. The more subdued shell textures among trionychids are easily distinguished from that in araripemydids. Nonetheless, araripemydids and trionychids share similarities in shell ornamentation, reduction or loss of scutes, and a relatively flat shell profile, all of which may constitute adaptations to an aquatic lifestyle.

Carapace: The *carapace* is complete except for a left portion of the posterior half that was broken away and lost upon discovery of the specimen. The carapace and plastron are in natural articulation with only minor disarticulation and dorsoventral crushing. Minor anteroposterior shortening has occurred with some imbrication of costals 3 and 4 and 7 and 8 (Fig. 14.11). Minor transverse flattening has occurred, creating gaps laterally at the plastral bridge and in the midline between the right and left hypo- and hyo-plastron (Fig. 14.13). When these postmortem distortions are removed, the carapace has a distinctly oval shape with two low convexities along the margin of peripherals 1–3 and greatest breadth at peripheral 7 (Fig. 14.2). The carapace in *Araripemys* differs from *Laganemys* with its more circular profile, deeper nuchal embayment, greater posterior extension relative to the hind limbs, presence of a series of fenestrae, and retention of a small ninth neural (Fig. 14.1).

In *Laganemys* the length of the carapace (144 mm) slightly exceeds its width (140 mm) as preserved (Table 14.1), and the vertical height within the shell appears to have been approximately 20 mm. The carapace, which has a thickness of approximately 1 mm, is composed of 1 nuchal, 11 paired peripherals, 8 neurals, 8 paired costals, 1 suprapygal, and 1 pygal (Figs. 14.2, 14.11).

The broad *nuchal* plate has a deep anterior embayment (Fig. 14.12). This feature is also present in *Araripemys* (Fig. 14.1) and is included among synapomorphies of Araripemydidae. The condition of *Laganemys* differs from *Araripemys* by retention of the primitive nuchal-peripheral 1 contact on the periphery of the carapace, which excludes costal 1 from the margin of the carapace. In *Araripemys* costal 1 forms a short section of the anterior margin of the carapace, separating the nuchal and peripheral 1. We regard the condition in *Araripemys* as an autapomorphy for the genus. The nuchal in *Laganemys* has a unique boomerang shape, with a transverse span equal to one-fourth the width of the carapace (Figs. 14.2, 14.11, 14.12). The broader nuchal embayment in *Araripemys* incorporates all of the margin of peripheral 1, the nuchal retaining a subtrapezoidal shape (Fig. 14.1). Gaffney et al. (2006) regarded nuchal shape in *Araripemys* as distinctive, along with its well developed sutural contact with the first dorsal vertebra. That contact is not currently exposed in *Laganemys*.

The *neural series* is limited to eight plates with a neural formula of $6 > 6 > 4 < 6 < 6 < 6 < 6 > 5$. Neural 7 is hexagonal with 6 sutural contacts. Neural 8 is very small and probably has 5 contacts (neural 7, costals 7, 8) (Fig. 14.2). *Araripemys* has a neural formula of $6 > 6 > 4 < 6 < 6 < 6 > 6 > 3$ and shows less reduction of the posterior neural series than *Laganemys*. All specimens of *Araripemys* have nine neurals, with neural 8 hexagonal and neural 9 small and triangular (Fig. 14.1). A comparison of neural formulae among basal pleurodires suggests that *Laganemys* has lost neural 9 and reduced the size of neural 8. Neural 3 in both *Laganemys* and *Araripemys* only has one costal contact (costal 3), although it retains a hexagonal shape (Figs. 14.1, 14.2). The hexagonal neural 3 in pelomedusoids, in contrast, maintains two costal contacts that subdivide its lateral margin ($4 < 6 < 6 < 6 < 6 < 6 < 6 < 6$). Neural 3 in *Laganemys* is noteworthy as well for its shape; its long axis is oriented transversely (Fig. 14.2). The neural and pygal series in *Laganemys* are separated by a substantial median contact between opposing costal 8 plates (Figs. 14.2, 14.11). In *Araripemys* intercostal contact at the posterior end of the neural series is variable. Some specimens show substantial median contact between opposing costal 8 plates equivalent to that in *Laganemys*, whereas in other specimens such contact is limited to the convergence of sutures to a point junction (Fig. 14.1; Meylan 1996). Intercostal contact separating the posteriormost neural and suprapygal is absent in *Euraxemys* but present in some pelomedusids, podocnemidids and bothremydids (Gaffney et al. 2006).

The *pygal series* consists of a single suprapygal and pygal. The single suprapygal plate in *Laganemys* and *Araripemys* (Figs. 14.1, 14.2, 14.11, 14.20) may represent a derived condition, as two suprapygals are present in the basal pleurodire *Notoemys* (Meylan 1996; Rueda and Gaffney 2005).

The *costal series* consists of eight plates, the first of which is much broader than the others as in *Araripemys*

(Fig. 14.1). The added breadth gives costal 1 a subtriangular shape, whereas costals 2–8 have subparallel anterior and posterior margins (Figs. 14.11, 14.12). Costal 8 meets its opposite in the midline as described above. The distal end of a dorsal rib projects from the distal margin of each costal plate, as seen in dorsal and ventral views of the carapace (Figs. 14.2, 14.3, 14.11). The distal ends of the ribs extending from costals 1–4 insert between peripherals, whereas the rib ends on costals 5–8 insert into a notch in the middle of the adjacent peripheral. Unlike the carapace of *Araripemys*, which has a series of small fenestrae between costal and peripheral plates (Fig. 14.1), the rib ends in *Laganemys* insert into the peripheral series closing all such gaps. The presence of fenestrae in the carapace in *Araripemys* cannot be attributed to immaturity, given their uniform presence in many specimens. Likewise, we regard the holotypic and only known specimen of *Laganemys* as a mature individual, given the fusion of all sutures in the vertebral column and the coossification or tight articulation of cranial sutures. The presence of fenestrae in the carapace in *Araripemys* and the broad extension of the posterior margin of the carapace may represent derived conditions and constitute additional specialization related to an aquatic lifestyle.

The first plate in the *peripheral series* is crescentic (Fig. 14.12). The other peripherals vary in shape: they are rectangular along the anterior margin (peripherals 2, 3), triangular where they are separated by a rib end (peripherals 3–5), subquadrate with a medial notch to accommodate a rib end (peripherals 7–10), and subquadrate (peripheral 11). The anterior margin of the carapace is scalloped with a convex edge formed by peripheral 1 and a second convexity at the junction of peripherals 2 and 3 (Fig. 14.2).

A lightly incised *scute pattern* is visible on the carapace, indicating the presence of 5 vertebral, 4 pleural and probably 12 marginal scutes, a common condition among turtles. The scutes, like the underlying peripherals, are reduced along the anterior margin of the carapace; there is no evidence for nuchal or supramarginal scutes anterior to the vertebral series in either *Araripemys* or *Laganemys* (Figs. 14.1, 14.2).

Dorsal vertebra 3 and 4 are exposed through the second plastral fenestra in ventral view of the shell (Fig. 14.13). These centra, approximately 14 mm in length, have a rounded ventral keel and tab-shaped processes extending from each side of the posterior end of the centrum.

Plastron: The plastron preserves all elements on one side or the other except for the distal tip of the xiphiplastron. Measuring 130 mm in length, the plastron nearly equals the length of the carapace (Table 14.1). The 11 bones of the plastron include an entoplastron and paired epi-, hyo-, hypo-, meso-, and xiphi-plastra. There are three median plastral fenestrae, the anterior two much larger than the posteriormost. The fenestrae are separated by plastral plates, which join along deeply interdigitating sutures (Figs. 14.3b, 14.13). The plastral bridge to the carapace spans nearly one-third the length of the plastron. Postmortem compression of the shell has disarticulated both axillary and inguinal buttresses (Fig. 14.13).

The *epiplastron* is a narrow strap-shaped plate, the posterior two-thirds of which lies at a 45° angle from the midline forming the lateral plastral margin alongside the ento- and hyo-plastron (Figs. 14.3b, 14.13). The posterior tip inserts into a notch in the hyoplastron. The anterior one-third of the element curves anteriorly to meets its opposite at the midline. The conjoined epiplastra project approximately 1 cm anterior to the entoplastron and approximately 2 cm anterior to the nuchal embayment on the carapace. In width (6 mm) and length (2 cm), the conjoined epiplastral projection roughly corresponds to that of a cervical centrum (Table 14.1). The broad nuchal embayment and opposing epiplastral process were probably involved in enhancing support or mobility of the long cervical series. A strap-shaped epiplastron is a synapomorphy of Araripemydidae. A J-shaped epiplastron is an autapomorphy of *Laganemys*.

The *entoplastron* is pointed anteriorly and posteriorly in the midline and has gently convex lateral margins, and a pointed posteromedian process extending into the anterior plastral fenestra. The bone thus is shaped like an arrowhead (Figs. 14.3b, 14.13). The entoplastron contacts the hypoplastron laterally along an interdigitating suture, the last notch of which accommodates a slender entoplastral prong. In *Araripemys* there is only a single broader prong inserting into a notch in the hyoplastron (Meylan 1996).

The *hyoplastron* forms most of the anterior one-half of the plastron, expanding anteriorly to meet the ento- and epiplastron and contributing to the lateral border of the anterior and middle plastral fenestrae (Figs. 14.3b, 14.13). The anterior edge of the hyoplastron has a concave embayment to accommodate the forelimb that extends posteriorly nearly as far as the posterior rim of the anterior plastral fenestra. The thickened lateral (axillary) buttress extends anteriorly along the lateral margin of the carapace as far as costal 1 and attaches to the middle of peripheral 3. The anterior margin of the buttress is smooth. The hyoplastra meet in the midline along a deeply interdigitating suture, separating anterior and middle plastral fenestrae. This suture is short (approximately 1 cm) with four triangular prongs of similar length (5 mm) on each side. Posteriorly the hyoplastron meets the hypo- and meso-plastron along an interdigitating suture.

The *mesoplastron* is a pentagonal plate located on the lateral margin of the plastral bridge between the hyo- and hypo-plastron (Fig. 14.3b). Its lateral margin contacts peripherals 5 and 6, and its medial apex is located between the hyo- and hypo-plastron. In *Laganemys* the mesoplastron

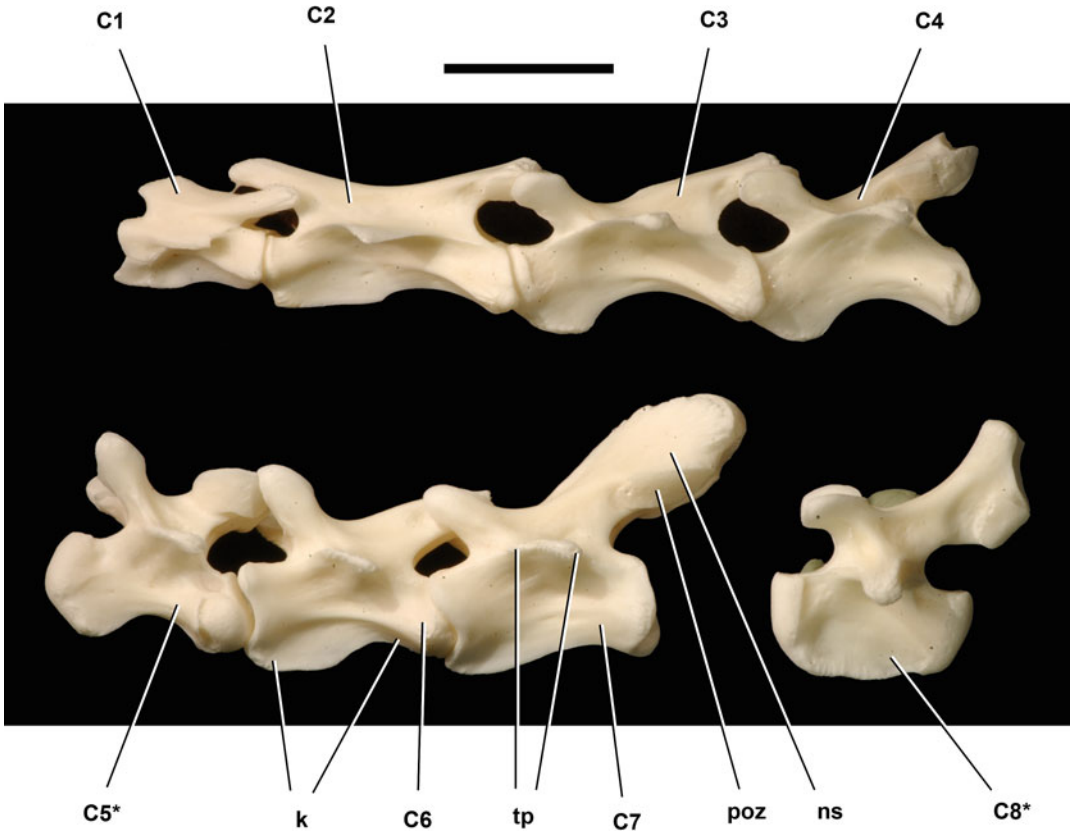

Fig. 14.19 Cervical vertebrae of the extant South American fringed turtle, *Chelus fimbriatus* (UCRC RV4), in lateral view. Asterisk indicates vertebrae with biconvex centra (C5, C8). Scale bar = 2 cm. Abbreviations: *C1–8* cervical vertebrae 1–8; *k* keel; *ns* neural spine; *poz* postzygapophyses; *tp* transverse process

is retained as a significant element of the plastron, forming approximately 30% of the plastral bridge (Fig. 14.3b). In *Araripemys*, in contrast, the mesoplastron is absent (Fig. 14.3a), although it is retained in many pelomedusoids.

The *hypoplastron* contacts the hyo- and meso-plastron anteriorly and xiphiplastron posteriorly along interdigitating sutures (Figs. 14.3b, 14.13, 14.14a, 14.23). The suture between the hypo- and xiphi-plastron runs from the posterior embayment to the posterior plastral fenestra. Except for an anterior marginal prong on the xiphiplastron, the suture between the hypo-, and xiphi-plastron is finely interdigitating, in contrast to the much longer interdigitating processes present in *Araripemys* (Fig. 14.3a). Like the hyo-, the hypo-plastron joins its opposite with six or seven triangular prongs of similar length (5 mm), separating middle and posterior plastral fenestrae. The posterior edge of the hypoplastron has a deeply concave embayment to accommodate the hind limb that extends anteriorly as far as the anterior edge of the posterior plastral fenestra. The posterior edge of the hypoplastron has a smooth margin that broadens as it approaches the lateral (inguinal) buttress, which extends as far posteriorly as peripheral 7 (Figs. 14.3b, 14.14a, 14.23).

The *xiphiplastron* forms the posterior one-fourth of the plastron, tapering in width posteriorly (Figs. 14.3b, 14.13, 14.23). The posterior palatal fenestra forms a narrow median fissure, separating the anterior one-third of the xiphiplastron from its opposite. More posteriorly, the xiphiplastron joins its opposite along a finely interdigitating median suture (Figs. 14.3b, 14.23). The posterior margin of the plastron follows a broad concave arc between prominent posterolateral corners of the xiphiplastra.

A lightly incised *scute pattern* is visible on the plastron that reveals the presence of scutes that once covered the plastron. In *Araripemys* a pair of anterior (humeral) scutes were reported on the anterior ends of the epiplastra (Fig. 14.3a; Meylan 1996), although later it was scored as a median intergular scute (Gaffney et al. 2006) as in extant turtles (Pritchard 1979). The most anterior scute on the plastron in *Laganemys* appears to be a median intergular scute (Fig. 14.3b.

Five pairs of scutes (humeral, pectoral, abdominal, femoral, anal; Pritchard 1979) cover the remainder of the plastron in both *Laganemys* and *Araripemys* (Fig. 14.3), although in some areas in *Laganemys* the scute margin is so faintly incised that it cannot be followed.

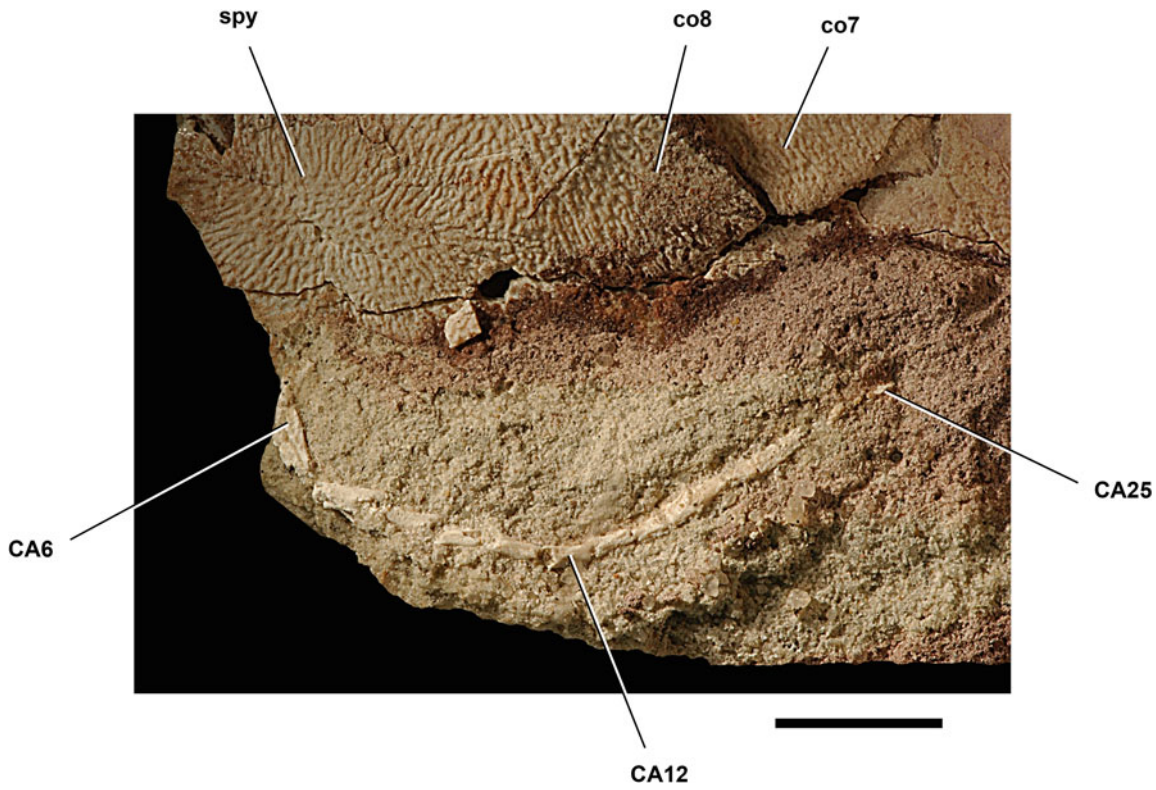

Fig. 14.20 Caudal vertebrae of *Laganemys tenerensis* gen. et sp. nov. (MNN GAD28) in dorsal view. Scale bar = 1 cm. Abbreviations: *CA6, 12, 25* caudal vertebra 6, 12, 25; *co7 8* costal 7, 8; *spy* suprapygal

Cervical vertebrae: The cervical vertebrae are preserved largely in articulation between the skull (removed during preparation) and the anterior hiatus of the shell. Cervical vertebrae 1, 2 and 4–7 are exposed in ventral view, whereas cervical vertebrae 3–6 and 8 are exposed in dorsal view.

The cervical vertebrae are joined along an S-shaped curve with greatest intervertebral angles between vertebrae with articular ends adapted for bending (Figs. 14.11, 14.13). The partially retracted position of the cervical series, thus, is a reflection of relative intervertebral mobility in life during retraction and extension of the head. The two vertebral joints with a high angle of excursion (approximately 90° cervicals 2 and 3; approximately 80°, cervicals 6 and 7) lie in transverse planes parallel to that of the shell as expected in a "side-necked" pleurodire. As in *Araripemys*, postatlantal cervical centra are elongate, roughly the same length, and approximately 25% longer than mid dorsal centra (Table 14.1). The cervical column in both *Araripemys* and *Laganemys* is approximately 90% of the midline length of the carapace, as measured from the nuchal embayment to the distal edge of the pygal (Figs. 14.1, 14.2).

The *atlas* has a short centrum approximately one-third the length of more posterior cervical centra. It has tab-shaped prezygapophyses, broad-based subtriangular postzygapophyses, and blunt transverse processes that rise from the base of the neural arch (Fig. 14.15). A low ridge is present on the dorsal edge of the prezygapophyseal process. The dorsal edge of the postzygapophysis is rugose for ligament attachment. The ventral aspect of the atlantal centrum is pinched anteriorly to form a low ventral keel. The form of the posterior centrum face is not well exposed but appears to be concave. The morphology of the atlas does not depart markedly from that in *Chelus* (Fig. 14.19).

The centrum of the *axis* is V-shaped in cross-section at mid length. A strong ventral keel arises at mid length along the centrum and gains in depth anteriorly, extending as a median prong under the atlantal centrum. The posterior portion of the axial centrum arches ventrally. The anterior face of the axial centrum is not well exposed but is probably convex and fitted to the concave posterior face of the atlantal centrum. The posterior face of the axial centrum is strongly convex. The axial centrum in *Laganemys*, thus, is biconvex, which also appears to be the case in *Araripemys* (Meylan 1996) and other pelomedusoids.

Broad-based, thin transverse processes projects from the anterior two-thirds of the axial centrum (Fig. 14.15). In dorsal view, the transverse process is subtriangular and broadest posteriorly. In lateral view, the transverse process is canted posteroventrally at its attachment to the neural arch and is deflected just below the horizontal as it extends laterally. The axial neural spine, like the ventral keel, arises

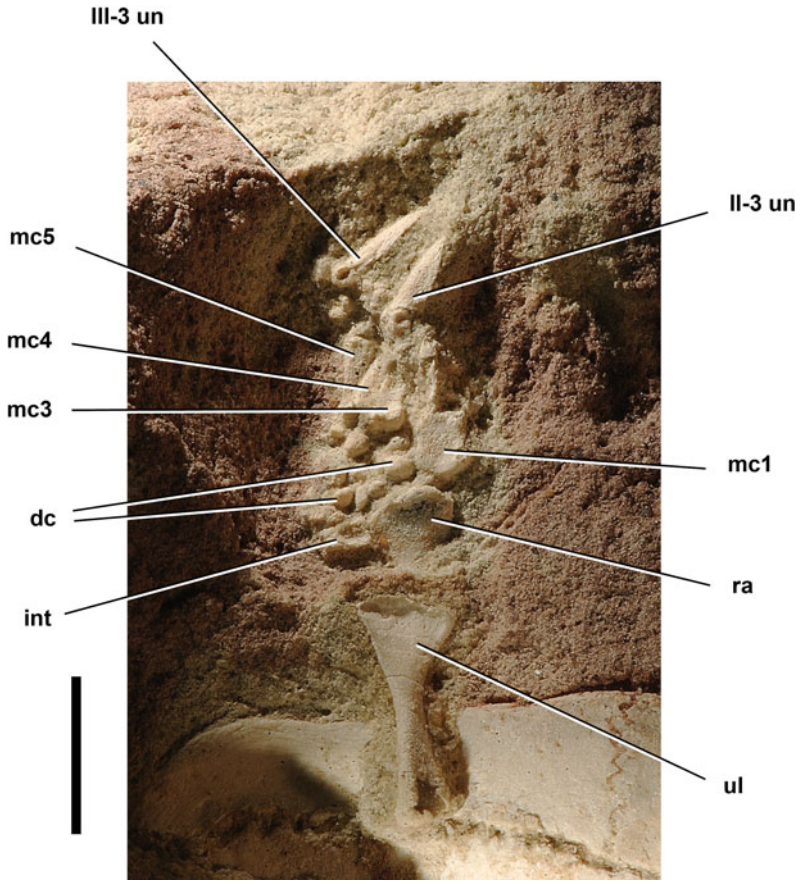

Fig. 14.21 Left forelimb of *Laganemys tenerensis* gen. et sp. nov. (MNN GAD28) in dorsal view. Scale bar = 1 cm. Abbreviations: *II*, *III* digit II, III; *dc* distal carpal; *int* intermedium; *mc1*, *3–5* metacarpals 1, 3–5; *ra* radius; *ul* ulna; *un* ungual

at mid length along the centrum and gains in depth anteriorly, extending as a median prong over the atlantal neural arch (Fig. 14.15). The prezygapophyses are flattened, laterally facing facets to each side of the prominent spine, the dorsal margin of which is slightly swollen.

The axial postzygapophyses are fused in the midline, forming a broad, horizontal fan-shaped process that encloses a subquadrate opening. This opening is largest in the axis. In postaxial cervicals 3–7, the opening is present as a smaller rounded foramen. Despite fusion of the postzygapophyses in cervical vertebrae 2–8, the articular facets themselves on the underside of the united process may remain separate; most of the articular facets are not fully exposed. The articular facet on the underside of the left axial postzygapophysis is exposed; it is flat, oval and separated from its opposite in the midline. The epipophyseal process originates as a low ridge on the dorsolateral aspect of the neural arch at mid length. The ridge gains in depth and width posteriorly, terminating as a posteriorly facing, wedge-shaped process, separated from its opposite by a median trough.

The centra of *postaxial cervical vertebrae* are procoelous, with the transverse concavity being stronger than the dorsoventral concavity (Figs. 14.15, 14.17). The anterior centrum face of cervical 7 is broader and more deeply concave from side to side than in other postaxial cervical vertebrae, enhancing the potential for transverse rotation of cervical 6. Cervical 6 as preserved is flexed at an angle of approximately 80° relative to cervical 7 (Fig. 14.18). The transverse diameter of the anterior face of cervical 7 (6 mm) is one-third greater than that of cervical 6 (4 mm), and its deeply concave articular surface is bounded to each side by a swollen articular rim. The posterior centrum face is convex but does not form a smooth ball in finished bone. In this regard, ossification seems less complete that in many other turtles. A ventral keel rises at mid length along the centra of the postaxial cervicals and increases in depth toward the anterior centrum face, which as a result has a subtriangular rather than circular shape. The ventral keel splits posteriorly into two rounded ridges that pass to the posteroventral corners of the posterior centrum face, resulting in an inverted subtriangular shape as in *Araripemys* (Meylan 1996). Cervical 7 has a well developed ventral keel that extends along the entire length of the centrum and is pendant anteriorly. A circular pit is present on the left side of the keel (Fig. 14.18).

In mid cervical vertebrae, a subtriangular transverse process extends horizontally from the base of the neural arch, projecting more prominently and extending farther posteriorly along the side of the centrum. In cervical 6, the

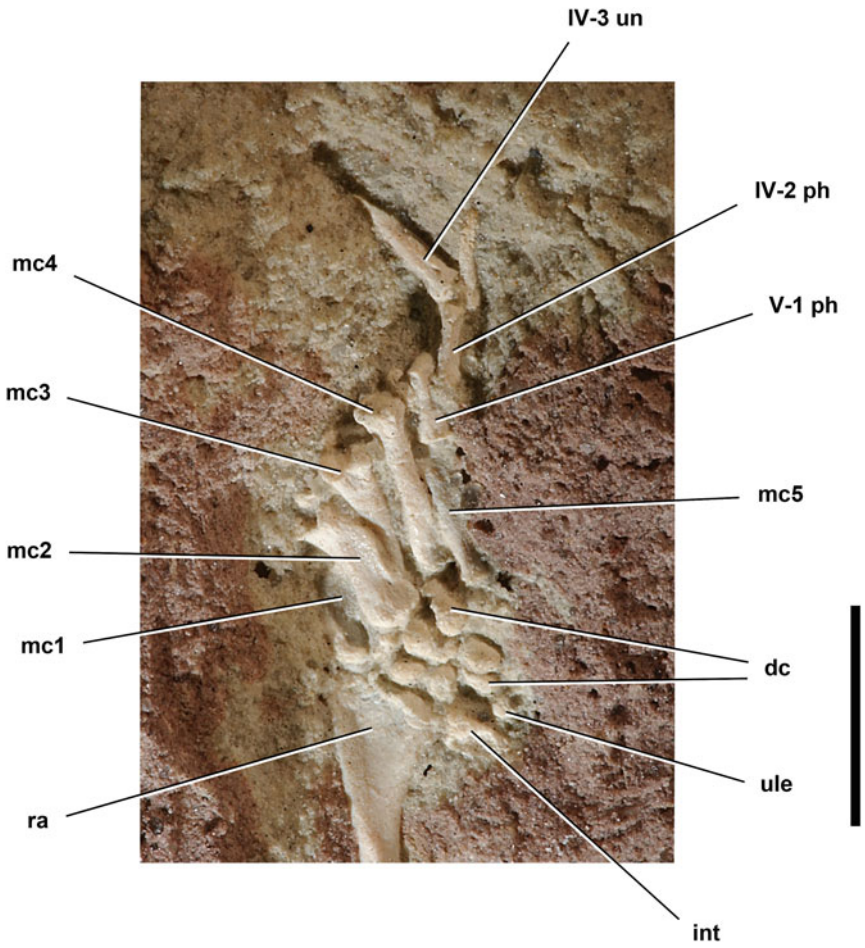

Fig. 14.22 Left carpus and manus of *Laganemys tenerensis* gen. et sp. nov. (MNN GAD28) in ventral view. Scale bar = 1 cm. Abbreviations: *IV, V* digit IV, V; *dc* distal carpal; *int* intermedium; *mc1–5* metacarpals 1–5; *ph* phalanx; *ra* radius; *ule* ulnare; *un* ungual

transverse process extends as a long subtriangular flange. In cervical 7 the anterior portion of the flange is reduced whereas the tip projects farther laterally (Fig. 14.18).

In mid cervical vertebrae, the neural spine is developed along the neural arch as a low crest that is strongest at mid length. The spine splits to each side of the midline posteriorly, forming the medial edge of wedge-shaped epipophyseal processes that are separated in the midline by a narrow groove. In postaxial cervicals, the epipophyseal process begins as a low ridge on the lateral aspect of the neural arch at mid length. The ridge forms the lateral margin of a broad, low epipophyseal process and joins the edge of the postzygapophysis. The flat, horizontal prezygapophyses of cervical 5 are exposed in articulation against the flat, conjoined postzygapophyses of cervical 4. Unlike the subdivided axial postzygapophyses, the articular surface of postaxial postzygapophyses extends without break across the underside of the subcircular, conjoined process.

The postzygapophyses on cervical 8 are separated distally by a median notch (Fig. 14.12). The epipophyses on cervical 8 are narrower and spaced farther from the midline than in other postaxial cervical vertebrae. In *Araripemys*, in contrast, the postzygapophyses of cervical 8 have been reconstructed as fully fused with broad, adjacent epipophyses and a small median foramen (Meylan 1996). In *Laganemys* postzygapophyses of this form are limited to cervical vertebrae 3–7. Fusion of the postzygapophyses characterizes *Euraxemys*, whereas the condition of the postzygapophyses in cervical 8 is variable in chelids and podocnemidids (Gaffney et al. 2006). The postzygapophyses are separate in pelomedusids and are widely spaced in the basal pleurodire *Notoemys* (Meylan 1996; Gaffney et al. 2006).

Dorsal vertebrae: The mid dorsal vertebrae are partially exposed through the plastral fenestrae (Fig. 14.13). Dorsal 4, which has been displaced ventrally through the middle fenestra, is the most visible. Centrum length decreases in the anterior portion of the dorsal series. The centrum of dorsal 2 is nearly as long as the postatlantal cervical centra, whereas the length of dorsal 4 is only approximately 75% the length of the cervical 7. The centrum of dorsal 4 is V-shaped in cross-section with a prominent, but rounded, ventral keel. It appears to be amphicoelous, although neither end is fully exposed. A dorsoventrally compressed parapophyseal process is present near the anterior end of the centrum and attaches to the head of the dorsal rib (Fig. 14.13). The anterior margin of the rib

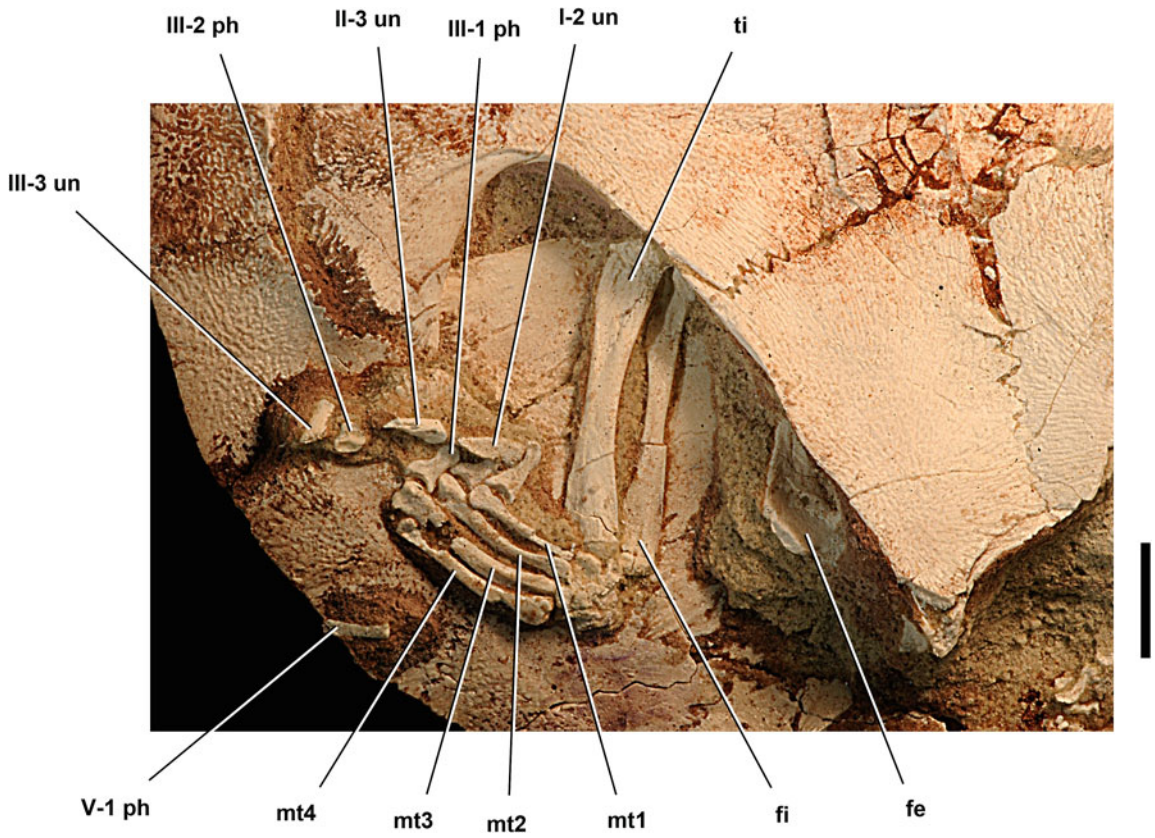

Fig. 14.23 Right distal hind limb of *Laganemys tenerensis* gen. et sp. nov. (MNN GAD28) with pes in ventral and lateral view. Scale bar = 1 cm. Abbreviations: *I–III*, *V* digits I–III, V; *fe* femur; *fi* fibula; *mt1–4* metatarsals 1–4; *ph* phalanx; *ti* tibia; *un* ungual

extends across the intervertebral joint to attach to a lateral flange projecting from the side of dorsal 3. The centra and keel of more anterior dorsal vertebrae are approximately one-half the depth of that in dorsal 4. The intervertebral attachment of the dorsal rib can also be seen in these vertebrae.

The dorsal vertebrae in *Laganemys* are proportionately longer than in *Araripemys* (Meylan 1996) and have projecting processes for attachment to the ribs. In *Araripemys* dorsal vertebrae 2–9 and their associated ribs are more fully incorporated into the carapace.

Caudal vertebrae: Most of the caudal series is preserved and exposed. The anterior caudal vertebrae are close to their natural position posterodorsal to the posterior embayment of the xiphiplastra (Fig. 14.13). Two anterior caudal vertebrae are exposed in ventral view; there may be a few additional caudal vertebrae embedded in the matrix closer to the sacrum. One of the exposed pair of anterior caudal vertebrae, tentatively identified as caudal 4, has a centrum length of 5 mm and a posterior diameter of 2 mm. This centrum is more elongate than comparable centra at the base of the tail in *Araripemys*, and the subtriangular transverse process is better developed (Meylan 1996). The articular faces of the centra are flat or slightly convex. The anterior caudal vertebrae, like those in mid and distal regions of the tail, are not procoelous as in pelomedusids. The transversely compressed centrum has a shallow median groove that diverges toward the posterior sides of the distal end, terminating in a pair of parasagittal prominences. Although these prominences are well positioned as articulations for haemal arches, no ossified chevrons are present as is also the case in *Araripemys* (Meylan 1996).

The remainder of the tail comprises an articulated series of 21 vertebrae that measure approximately 45 mm in length (Fig. 14.20). This portion of the tail has been displaced anterodorsally, so its proximal end lies dorsal to the pygal plate. The first caudal in this section of the tail is estimate to be caudal 6; the series tapers in diameter, terminating in a tiny nubbin of bone representing caudal 26. Caudal 20 is missing, a gap of appropriate length in its place in the otherwise articulated series.

The tail is longer in *Laganemys* than *Araripemys* (Figs. 14.1, 14.2). It extends well beyond the posterior margin of the carapace. Tail length has been augmented in *Laganemys* by increasing the number and length of caudal vertebrae (Table 14.1). In *Araripemys* there are less than 20 caudal vertebrae, whereas in *Laganemys* there are at least 26 caudal vertebrae. In mid and distal caudal vertebrae in *Laganemys*, the centra have lengths between two and three times

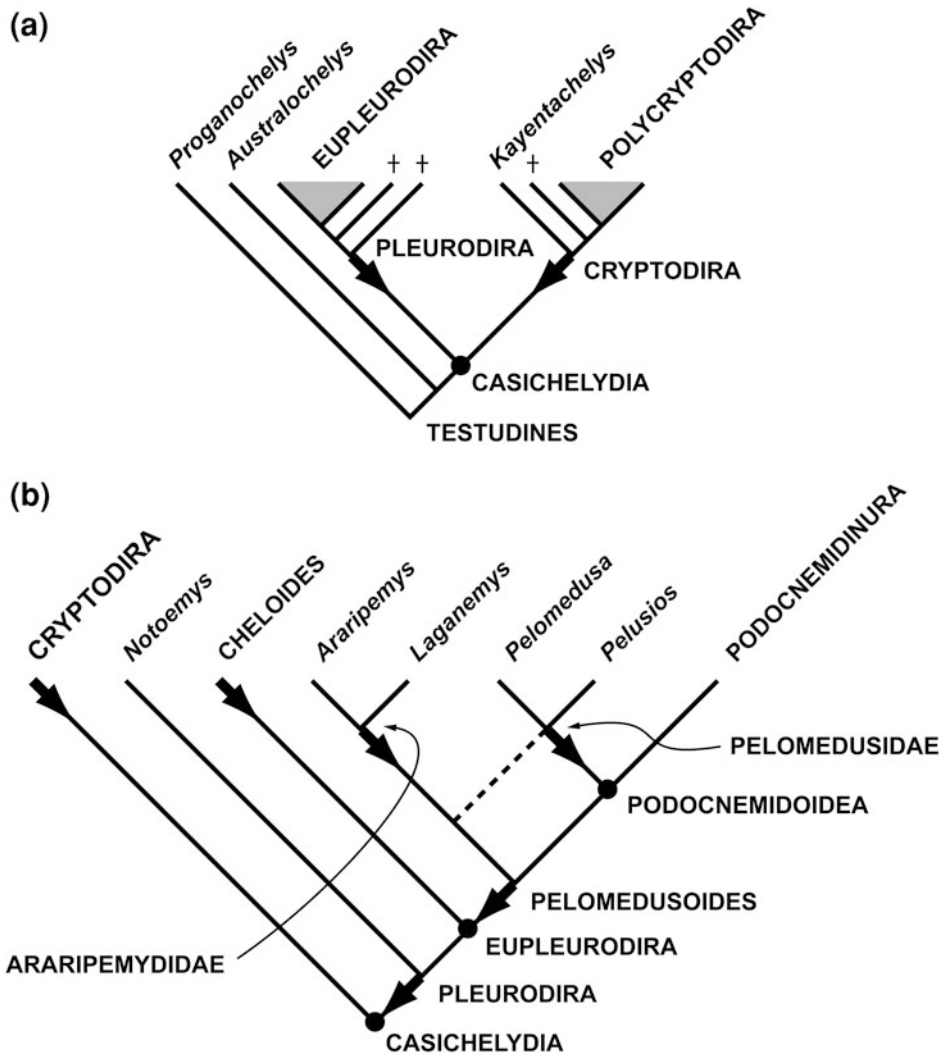

Fig. 14.24 **a** Suggested node-stem triplet of phylogenetic definitions to stabilize the meaning of higher taxa as had long been effected in classifications by Gaffney (from Sereno 2005). **b** Cladogram showing the phylogenetic relationships of araripemydid turtles within Pleurodira, based on reanalysis of data in Gaffney et al. (2006). *Dashed line* in **b** indicates a slightly less parsimonious position for Araripemydidae. *Dots* indicate node-based definitions; *arrows* indicate stem-based definitions; *daggers* indicate extinct taxa; *tone* indicates crown pleurodires and crown cryptodires (see Table 14.2 for phylogenetic definitions)

centrum diameter, whereas they appear to have subequal dimensions in *Araripemys* (Meylan 1996). Zygapophyseal articulations angle ventromedially at approximately 45–60° in *Laganemys* and are present in posterior caudal vertebrae back to approximately caudal 20, after which the centra are little more than cylinders. There are no neural spines in mid and distal caudal vertebrae.

Forelimb: The left radius and ulna, carpus and manus are preserved extending from the plastral embayment for the forelimb (Figs. 14.21, 14.22). The humerus is not present, and the edge of peripheral 2 is inserted between the proximal ends of the radius and ulna. This portion of the forelimb, thus, is partially disarticulated with some distal displacement of the radius, carpus and manus relative to the ulna. The preserved orientation of the forearm and manus, nevertheless, is typical of extant aquatic turtles. The forearm and manus in most turtles is capable of a palm-down orientation with the pollex on the medial side of the manus (Figs. 14.1, 14.2). In many aquatic turtles, however, supination at the elbow reverses the position of the forearm and manus to a posterior and palm-up position, respectively. This is the case in the holotypic specimen of *Laganemys*. The left manus is in ventral view (palm-up) with the pollex on its lateral side when looking down on the carapace (Figs. 14.11a, 14.20).

The *radius* is fully exposed in ventral (anterior) view (Figs. 14.13, 14.22). Like the ulna, its proximal end is considerably narrower than the paddle-shaped distal end, which is relatively more expanded than in *Araripemys* (Meylan 1996). The distal end expands to a width of 6 mm, or approximately 40% of radial length (Table 14.1). The proximal end appears to have a shallow saddle-shaped articular surface for the medial humeral condyle, and the shaft narrows slightly in mid section. In *Araripemys*, in contrast, the radial shaft does not narrow appreciably in mid section, and a prominent ridge is developed along the medial side of the shaft and distal end (Meylan 1996). In *Laganemys* the ventral (posterior) aspect of the distal end

is marked by a shallow subtriangular fossa (Fig. 14.22). The distal end is beveled mediodistally at a greater angle (approximately 60°) to the long axis of the radius than in *Araripemys* (Meylan 1996). The distal end contacts the intermedium, two distal carpals, and the base of metacarpal 1, although some postmortem shifting among carpals may have occurred (Figs. 14.21, 14.22).

The proximal end of the *ulna* is more expanded than that of the radius and has a fossa on its dorsal (posterior) side (Fig. 14.21). The distal end expands to a width of 7 mm, or approximately 45% of ulnar length (Table 14.1). The distal end is more symmetrical than that of the radius. A shallow fossa is present above the distal end, which is gently beveled laterodistally at an angle of approximately 85° to the long axis of the ulna.

The *carpus* is composed of a large wedge-shaped intermedium, an ellipsoidal ulnare, and six flattened or ovoid carpals, as best seen in ventral view (Fig. 14.22). The intermedium has a concave medial facet fitted to the lateral distal corner of the radius and thus appears to be in place. The ventral aspect of both the intermedium and ulnare are concave with a finished nonarticular surface of periosteum facing ventrally. A similar set of carpal elements were described in *Araripemys*, but only five carpals were shown in reconstruction, these being interpreted as distal carpals 1–5 (Meylan 1996). The specific identity of the distal six carpals in *Laganemys* is uncertain, as they are not positioned in sequence in direct association with individual metacarpals (Figs. 14.21, 14.22).

The *metacarpals* are the longest bones in each of the five manual digits, and digit IV and metacarpal 4 are the longest digit and metacarpal in the manus, respectively, as in *Araripemys* (Figs. 14.1, 14.2, 14.21, 14.22, Table 14.1). In *Laganemys* as in *Araripemys*, the forearm and manus have similar proportions relative to one another; the radius is 76 versus 73% of the length of digit IV in *Laganemys* and *Araripemys*, respectively. The phalanges, however, comprise a greater proportion of manual length in *Laganemys* than in *Araripemys*; metacarpal 4 is 50 versus 66% of radial length, respectively, whereas metacarpal 4 is 62 versus 91% of the length of the phalanges in digit IV, respectively (Table 14.1). Individual phalanges, likewise, have more elongate proportions in *Laganemys* (Fig. 14.22). The first phalanx in manual digits I–IV is considerably longer than broad in *Laganemys*, whereas these proximal phalanges have subquadrate proportions in *Araripemys* (Meylan 1996). The unguals in *Laganemys*, likewise, taper from a subcylindrical proximal articular surface to flattened distal apices, whereas in *Araripemys* the unguals are shaped like arrowheads with distinctive prongs on each side for the ungual sheath. Thus, the nonterminal and ungual phalanges in *Laganemys* comprise a greater proportion of manual length and are relatively more slender than in *Araripemys*.

Mid-shaft diameter decreases from metacarpal 1 to 5, the former stout and dorsoventrally compressed and the latter slender and rod-shaped (Fig. 14.22). Although *Araripemys* shows this lateral decrease in metacarpal diameter, it is more striking in *Laganemys*. Metacarpal 1, for example, has very stout proportions, its mid-shaft width (4 mm) 60% of its length (6 mm). In *Araripemys* the mid-shaft width of metacarpal 1 is only approximately 40% of its length. The base of metacarpal 1 in *Laganemys* is V-shaped in dorsal view, and the broad shaft is transversely concave (Fig. 14.22). Portions of the distal condyles were lost during preparation.

Metacarpal 2 has a characteristic shape, similar to, but more strongly expressed, than in *Araripemys* (Meylan 1996). There is a distinctive lateral buttress along the proximal two-thirds of the metacarpal, distal to which the divided metacarpal condyles are deflected medially (Fig. 14.22). We regard the flange-like lateral buttress on metacarpal 2 as a synapomorphy uniting araripemydids. We regard the strong medial deflection of the distal condyles as an autapomorphy of *Laganemys*. As far as we are aware, the condition of metacarpal 2 in araripemydids is unique among turtles (Gaffney 1990). Proximal to the lateral buttress, there is a subtriangular overlap facet for the base of metacarpal 3. When metacarpal bases overlap *en echelon* in turtles, this occurs from medial to the lateral side of the metacarpus as seen in dorsal view (Gaffney 1990). Thus, the base of metacarpal 2 should overlap that of metacarpal 3 in natural articulation, not the reverse as shown in the reconstruction of the manus in *Araripemys* (Meylan 1996, Fig. 10A).

The proximal end of metacarpal 3 is dorsoventrally compressed. Its distal end is broader than deep and has divided condyles with a saddle-shaped articular surface for the proximal phalanx (Fig. 14.22). Metacarpal 4 also has a dorsoventrally compressed base, but its distal end is subquadrate and only weakly divided into condyles for articulation with the proximal phalanx. Metacarpal 5 appears to have a subquadrate base but flattens dorsoventrally toward its single distal articular condyle.

The *phalanges* in the manus compose a formula of 2-3-3-3-3 as is common among subaquatic turtles. In manual digit I, the medial one-half of the first phalanx and most of the ungual was lost during preparation. In each manual digit, the proximal phalanx is shorter than the second phalanx. All nonterminal manual phalanges have articular ends that are broader than deep, divided condyles, and well formed collateral ligament pits. All manual digits terminate with slender, gently arched unguals with dorsoventrally flattened tips that would have borne horny ungual sheaths (Figs. 14.21, 14.22). Although Meylan (1996) suggested the terminal phalanx of manual digit V was not covered with an ungual sheath in *Araripemys*

(Fig. 14.1), in *Laganemys* its form is similar to that of the other terminal phalanges (Fig. 14.2). We suspect that in both genera it was clawed in life in a fashion similar to manual digits I–IV.

Hind limb: The right hind limb is preserved largely in articulation extending from the plastral embayment. The proximal end of the femur is exposed under the lateral edge of the xiphiplastron and extends anteriorly within the shell. The bones of the crus are exposed within the plastral embayment in ventral (posterior) view, with the fibula medial to the tibia. The pes is pressed against peripherals 8 and 9 and exposed in ventral and medial views (Fig. 14.23). The tarsus and metatarsal 5 are poorly preserved, and the phalanges of digit IV and all but part of the proximal phalanx of digit V are missing. Pedal digits I and II are flexed and preserved in articulation. The distal two phalanges of pedal digit III are displaced approximately 1 cm from the proximal phalanx, and a portion of the proximal phalanx of digit V is displaced approximately 2 cm to the edge of the carapace.

The *tibia* is not bowed as in *Araripemys* (Meylan 1996) but rather tapers in width from lateral and medial sides toward the mid-shaft (Fig. 14.23). The medial margin of the shaft of tibia in *Laganemys* is slightly concave rather than convex as in *Araripemys*. An elongate subtriangular fossa is present on the ventral (posterior) aspect of the proximal end of the tibia. The distal end is rounded with a deep articular surface for the astragalus. The *fibula* is more slender relative to the tibia and more constricted at mid-shaft than in *Araripemys* (Meylan 1996). Its maximum mid-shaft diameter (2 mm) is one-half that of the maximum width of either the proximal or distal ends.

The *metatarsals* are the longest bones in pedal digits I–IV, and digit III and metatarsal 3 are the longest digit and metatarsal in the pes as in *Araripemys* (Figs. 14.1, 14.2, 14.23, Table 14.1). The metatarsals are flattened dorsoventrally with *en echelon* overlap of their proximal ends. Metatarsal 1 has rotated so that the narrow lateral side of its shaft is facing dorsally (Fig. 14.21). Metatarsals 1–3 have transversely broad, divided distal condyles, whereas metatarsal 4 has a narrower single distal condyle. Metatarsals 2 and 4 are subequal in length.

The *phalanges* in the pes compose a formula of 2-3-3-?-?, a count for the inner digits that is widespread among turtles (Gaffney 1990). The pedal unguals are broader and more dorsoventrally compressed than those in the manus but similar in form, lacking well formed lateral processes for attachment of the ungual sheath. In *Araripemys* the pedal unguals are shown as increasing in length from digits I to IV (Meylan 1996). In *Laganemys*, in contrast, the longest ungual is on pedal digit I, with progressively shorter unguals on pedal digits II and III (Figs. 14.2, 14.23).

Phylogenetic Position

Higher Level Taxonomy Within Pleurodira

The meaning of suprageneric taxon names at the base of Pleurodira is important, given an increasing number of extinct genera and hypotheses of relationship. Classifications of pleurodiran turtles using Linnaean categorical ranks have been around for more than a century and have survived recent revolution in systematic methods (Gaffney 1984; Broin 1988; Gaffney et al. 2006). Phylogenetic systematists (e.g., Hennig 1966), nonetheless, long have questioned the utility of ranks and redundant taxa, and a school of "phylogenetic taxonomy" has emerged that defines taxa on the basis of phylogenetic relationships (de Queiroz and Gauthier 1990, 1992). Additional conventions have been proposed, such as allying "commonly used" higher taxa with crown clades, and these conventions have been applied to turtle taxonomy (Joyce et al. 2004).

Both traditional and phylogenetic approaches, ironically, have generated turtle taxonomies that seem to dwell as much on excess as utility. Gaffney et al. (2006) erected a taxonomy for pleurodires rife with new ranked suprageneric taxa of questionable use, such as "Parvorder Minipleurodira" and "Subtribe Nigeremydina," many of which label poorly supported nodes. In their best-case phylogenetic scenario (with eight "shell-based" genera eliminated), many of the new or resurrected suprageneric taxa have no home on a consensus tree summarizing 590 equally parsimonious trees—just two steps beyond their preferred 382-step minimum-length cladogram. "Magnafamily Pelomedusera", in addition, contains taxa (Araripemydidae, Pelomedusidae) that are not sister taxa on their preferred cladogram.

The rank-free phylogenetic scheme erected by Joyce et al. (2004; Joyce 2007), on the other hand, restricts Pleurodira to crown members (the largest clade bounded by extant taxa), with "Panpleurodira" erected as an unwelcome replacement for Pleurodira in classifications such as Gaffney et al. (2006). Pelomedusoides is also recognized as a crown group (for Pelomedusidae + Podocnemidae) by excluding stem taxa. These stem taxa, however, were included when this taxon was coined (Broin 1988) and in subsequent usage (Meylan 1996; Gaffney et al. 2006). As before, a new taxon "Panpelomedusoides" was coined as a replacement to accommodate the ousted stem taxa. In this way, the traditional use of higher taxa that include extinct species is sacrificed to define taxa on present-day survivors.

Many turtle taxonomists have taken a "wait-and-see" approach in response to these conflicting taxonomic

Table 14.2 Phylogenetic definitions for Casichelydia (crown turtles) and principal higher level taxa within Pleurodira utilizing node-stem triplets for nomenclatorial stability (Fig. 14.24b)

Taxon	Definitional type	Phylogenetic definition
Casichelydia Gaffney 1975	Node (crown clade)	The least inclusive clade containing *Pelomedusa subrufa* (Bonnaterre 1789) and *Testudo graeca* Linnaeus 1758
Cryptodira Cope 1868	Stem	The most inclusive clade containing *Testudo graeca* Linnaeus 1758 but not *Pelomedusa subrufa* (Bonnaterre 1789)
Pleurodira Cope 1865	Stem	The most inclusive clade containing *Pelomedusa subrufa* (Bonnaterre 1789) but not *Testudo graeca* Linnaeus 1758
Eupleurodira Gaffney and Meylan 1988	Node (crown clade)	The least inclusive clade containing *Chelus fimbriatus* (Schneider 1783), *Pelomedusa subrufa* (Bonnaterre 1789), *Podocnemis expansa* (Schweigger 1812)
Cheloides Gray 1825	Stem	The most inclusive clade containing *Chelus fimbriatus* (Schneider 1783) but not *Pelomedusa subrufa* (Bonnaterre 1789), *Podocnemis expansa* (Schweigger 1812)
Pelomedusoides Broin 1988	Stem	The most inclusive clade containing *Pelomedusa subrufa* (Bonnaterre 1789), *Podocnemis expansa* (Schweigger 1812) but not *Chelus fimbriatus* (Schneider 1783)
Araripemydidae Price 1973	Stem	The most inclusive clade containing *Araripemys barretoi* Price 1973 but not *Chelus fimbriatus* (Schneider 1783), *Pelomedusa subrufa* (Bonnaterre 1789), *Podocnemis expansa* (Schweigger 1812)
Podocnemidoidea Cope 1868	Node (crown clade)	The least inclusive clade containing *Pelomedusa subrufa* (Bonnaterre 1789), *Podocnemis expansa* (Schweigger 1812)
Pelomedusidae Cope 1868	Stem (crown clade)	The most inclusive clade containing *Pelomedusa subrufa* (Bonnaterre 1789) but not *Podocnemis expansa* (Schweigger 1812)
Podocnemidinura Cope 1868	Stem	The most inclusive clade containing *Podocnemis expansa* (Schweigger 1812) but not *Pelomedusa subrufa* (Bonnaterre 1789)

Dagger marks higher taxa without extant representatives. Commas between author and year are omitted in phylogenetic definitions to avoid confusion (Sereno 2005)

schemes (Bickham et al. 2007). An alternative way forward has advocated the use of phylogenetic definitions to reflect and stabilize, rather than reorganize, the phylogenetic content in traditional classificatory schemes (Sereno 2005). If, for example, Pleurodira and Cryptodira long have been recognized as subclades of Casichelydia (Gaffney et al. 1987), complementary phylogenetic definitions can stabilize that relationship. A heuristic phylogenetic taxonomy can reduce present and future ambiguity regarding the taxonomic content of traditional suprageneric taxa, such as Araripemydidae.

For our subsequent discussion of relationships, we provide phylogenetic definitions for a higher taxonomy of Pleurodira (Fig. 14.24b, Table 14.2), building on the definition of Pleurodira initially proposed in Sereno (2005) (Fig. 14.24a). This taxonomy stabilizes three widely recognized dichotomies with phylogenetic definitions formulated as node-stem triplets: Casichelydia = Pleurodira + Cryptodira; Eupleurodira = Cheloides + Pelomedusoides; Podocnemidoidea = Pelomedusidae + Podocnemidinura. We do not recommend the use of Pelomedusoidea or Podocnemoidae as in Meylan (1996); the former taxon may engender confusion with Pelomedusoides in the vernacular ("pelomedusoids"), and the latter is redundant with Podocnemidinura as used in Gaffney et al. (2006). Contrary to Joyce et al. (2004), we recognize a stem-based Pelomedusoides to reflect its consistent use in the literature. Likewise, we recommend use of the vernacular "pelomedusoids" for Pelomedusoides, as is common in the literature and as used in the present paper. The proposed definitions also respect the hierarchy of suffixes recommended in traditional taxonomy (ICZN 1999).

Relationships Among Basal Pleurodires

Once the morphology of *Araripemys barretoi* became better known, its status as a basal pleurodire has not been questioned (de Broin 1980, 1988; Meylan and Gaffney 1991; Hirayama 1991). Among extant pleurodires, *Araripemys* has always been considered to be closer to Podocnemidoidea than Chelidae. The basic question is where *Araripemys*—or now the Araripemydidae—is positioned relative to podocnemidoid pleurodires (Fig. 14.24b). Does Araripemydidae lie outside all podocnemidoids, or is it more closely related to pelomedusids?

Meylan (1996) and Gaffney et al. (2006) considered the position of *Araripemys barretoi* among basal pleurodires. Both analyses placed *Araripemys* outside Podocnemidoidea as the basal sister taxon within Pelomedusoides (Fig. 14.24b). Meylan's (1996) analysis was based on 35 characters in *Araripemys* and 14 other pleurodire taxa (6 extant taxa, 8 extinct), for which he reported 5 minimum-

length trees of 56 steps. He cited three synapomorphies that unite Podocnemidoidea to the exclusion of *Araripemys*: (1) neural-suprapygal contact eliminated by median intercostal contact; (2) closure of the incisure of the columella auris; and (3) frontal interorbital suture transverse rather than anteriorly pointing.

Rerunning the data matrix shows that only 32 of the 35 characters are parsimony-informative (27, 32 and 34 are uninformative) and that there are 8 rather than 5 minimum-length trees of 56 steps. The topology near *Araripemys*, nonetheless, is as reported by Meylan (1996). However, only the first two of the three characters he cited as synapomorphies supporting this topology are in the character list and matrix. Indeed, the basal position of *Araripemys* within Pelomedusoides is based entirely on these two synapomorphies (characters 22, 35); two additional steps are required to collapse this node.

In the data matrix of Meylan (1996), several characters are scored incorrectly for *Araripemys*. These include jugal–quadratojugal contact (character 2; present rather than absent), the presence of a vomer (character 3; unknown rather than present), and presence/size of the mesoplastron (character 27; absent rather than unknown). In addition, we added *Laganemys* to this matrix to determine its affect, as it differs from *Araripemys* in character state scores in four characters (characters 2, 14, 27, 33). Rerunning the matrix with adjusted data for *Araripemys* and/or including *Laganemys* does not alter the key results of the analysis by Meylan (1996); two synapomorphies that are absent in *Araripemys* (and now also *Laganemys*) support the basal position of Araripemydidae within Pelomedusoides.

Gaffney et al. (2006, Fig. 288) obtained a similar topology with *Araripemys* as the basal taxon within Pelomedusoides based on a larger matrix of 175 characters in *Araripemys* and 40 other taxa, for which they reported a single minimum-length tree of 382 steps. One additional step collapses the basal position of *Araripemys* within Pelomedusoides. There was no discussion of the character evidence, however weak, for the basal position of *Araripemys* within Pelomedusoides. Rather Gaffney et al. (2006, p. 653) highlighted a synapomorphy of Podocnemidinura absent in both *Araripemys* and Pelomedusidae—the partial or complete covering of the prootic by adjacent cranial bones (character 94). This character, however, is not a synapomorphy supporting Podocnemidinura in their analysis as they noted elsewhere. This overlapping three-state character was left unordered, and as a result the two derived states optimize at nodes other than Podocnemidinura on either of their preferred cladograms (Gaffney et al. 2006, Figs. 288, 292). A second shortest tree was obtained after addition of eight "shell-based" taxa with character data largely limited to the shell; *Araripemys* now joins Pelomedusidae as the sister clade to Podocnemidinura within Podocnemidoidea (Fig. 14.24b, dashed lines). The character evidence supporting this relationship also was not discussed.

Araripemydidae as Basal Pelomedusoids

From the above it is clear that the precise position of *Araripemys* and the Araripemydidae among basal pleurodires is poorly established. The following questions remain:

(1) Which characters unite Podocnemidoidea to the exclusion of Araripemydidae in the analysis of Gaffney et al. (2006)?
(2) What happened to the pair of synapomorphies that functioned in this manner in the earlier analysis of Meylan (1996)?
(3) What is the character evidence that links *Araripemys* and Pelomedusidae, when "shell-based" taxa are added to the analysis?
(4) What effect, if any, does a second well preserved araripemydid, *Laganemys*, have on phylogenetic resolution?

Question 1. In the analysis of Gaffney et al. (2006), three homoplastic characters weakly unite Podocnemidoidea to the exclusion of *Araripemys*: procoelous caudal vertebrae (character 129); carapace with nuchal embayment (character 154); and a small, laterally positioned mesoplastron (character 158). *Laganemys* confirms the absence of procoelous caudal vertebrae in araripemydids. The evolution of procoelous caudal vertebrae, however, has an ambiguous distribution on the shortest tree (Chelidae, Pelomedusidae + Podocnemoidae). Procoelous caudal vertebrae thus might have evolved earlier within Pleurodira only to have been lost in araripemydids. Indeed, this is the optimization of this character when "shell-based" taxa are added to the analysis. A third poorly defined character state ("formed centra, but articulations vary") was also listed for character 129; perhaps fortunately, no taxa were scored with this condition.

The nuchal embayment (character 154) evolved or has been lost half a dozen times in the analysis (Gaffney et al. 2006); in the shortest tree, it is optimized as an unambiguous reversal uniting Podocnemidoidea. When additional "shell-based" taxa are added to the analysis, the supporting reversal no longer exists. This character does not provide convincing support.

The coding and optimization of states regarding the mesoplastron (character 158) are problematic. This four-state character is a coding chimera (Sereno 2007). "Absent" is mixed with two shape states (rectangular, equidimensional) and one based on topology (median contact). The

supporting transformation for Podocnemidoidea in the shortest tree is a partial reversal, the reappearance of a small mesoplastron. To make matters more homoplastic, *Laganemys* has a small mesoplastron (absent in *Araripemys*). When "shell-based" taxa are added to the analysis, mesoplastron transformations do not lend any support for Podocnemidoidea, so this character does not maintain a basal position for Araripemydidae within Pelomedusoides.

Question 2. The pair of podocnemidoid synapomorphies cited by Meylan (1996) is listed as characters 52 and 141 in Gaffney et al. (2006). Closure of the incisure of the columella auris now has three states (character 52). The condition is open in Araripemydidae, as confirmed in *Laganemys* (Fig. 14.4). The main difference in this connection is that Meylan (1996) scored chelids as having an open incisure, whereas Gaffney et al. (2006) described a closed incisure for chelids, eliminating the possibility this character could function as a podocnemidoid synapomorphy.

Meylan (1996) highlighted the loss of neural–suprapygal contact as a podocnemidoid synapomorphy absent in *Araripemys*, and Gaffney et al. (2006) scored *Araripemys* as primitive in this regard (character 141). Meylan (1996), nonetheless, described the condition in *Araripemys* as variable, some specimens showing broad costal contact between the last neural and suprapygal as in *Laganemys* (Figs. 14.2, 14.11). Gaffney et al. (2006) scored *Araripemys* as primitive (neural–suprapygal contact present) and parsed the character into four overlapping states of increasing costal contact. Despite the possibly erroneous character state score for *Araripemys* (Fig. 14.1), no transformation of this character, whether ordered or not, unites podocnemidoids over *Araripemys* on their preferred tree.

Question 3. With "shell-based" taxa added to the matrix, two unambiguous synapomorphies support *Araripemys* + Pelomedusidae (Gaffney et al. (2006, Fig. 292), namely, extreme temporal emargination (character 14) and hypoplastron–costal 1 contact (character 148). Derived temporal emargination is homoplasious, appearing four times independently in pleurodires as noted by Gaffney et al. (2006). *Laganemys* (Fig. 14.4), like *Araripemys*, has deep temporal emargination, but it would not be scored as such by their criterion (narrow orbit-to-temporal distance). Contact between the hyoplastron and costal 1 is a three-state coding chimera (Sereno 2007). The absence of contact is mixed with the two states describing where contact occurs in some taxa. The supporting synapomorphy is a reversal from one of these states of contact to absence of contact in *Araripemys*, although the condition in pelomedusids is scored as variable. This character cannot be observed in *Laganemys* and is missing in more than half of the taxa in the analysis. In sum, it is not surprising that the link between *Araripemys* and Pelomedusidae collapses with one additional step in tree length.

Question 4. Adding *Laganemys* to the analysis of Gaffney et al. (2006), either with or without "shell-based" taxa, results in a slight decrease in resolution regarding the position of Araripemydidae (see Appendix for character state scores). When reanalyzed without "shell-based" taxa, two polytomies (six minimum-length trees) are present, one of which involves Araripemydidae, Pelomedusidae and Podocnemidoidea. When "shell-based" taxa are added, there is similarly no resolution between these same three taxa. While *Laganemys tenerensis* has increased our knowledge of Araripemydidae, it has not helped to resolve the relationship of the family in the context of available phylogenetic studies.

Phylogenetic Resolution

The description of *Laganemys tenerensis* has brought to light considerable new evidence regarding the unique morphology of an unusual transAtlantic clade of aquatic pleurodires. The relationship between *Laganemys* and *Araripemys* is strong, even before the many new synapomorphies listed in the above diagnoses are added to the analysis. While the family rests comfortably within Pelomedusoides among basal pleurodires (Fig. 14.24b), resolution of its relationship with two other major clades within Pelomedusoides (Pelomedusidae, Podocnemidoidea) is not possible based on available data. This circumstance may persist, given the completeness of araripemydid material, until other basal pleurodires come to light.

Biogeographic Significance

Intercontinental vicariant events during the Cretaceous have been proposed to account for the transAtlantic distribution of well known extant pelomedusoid pleurodires, namely the pairs of closely related genera *Pelusios* and *Pelomedusa* on Africa and the genera *Peltocephalus* and *Podocnemis* on South American (Baur 1993). The fifth and last extant pelomedusoid genus, *Erymnochelys*, resides on Madagascar and is most closely related to the South American pelomedusoids (Gaffney and Meylan 1988; Noonan 2000). Although this Madagascar-South America connection has been cited as evidence against large-scale transAtlantic vicariance (Noonan 2000), one potential paleogeographic scenario for the break-up sequence of Gondwana envisions the early geographic isolation of Africa from other southern land areas, including South America and Madagascar

("Africa-first" hypothesis; Sereno et al. 2004; Sereno and Brusatte 2008).

Much more problematic for a vicariant explanation for extant pelomedusoid distribution is the widely distributed clade of extinct bothremydids, which lie outside Podocnemidinura, the clade including the South American genera *Peltocephalus* and *Podocnemis* (Fig. 14.24b; Noonan 2000; Gaffney et al. 2006). Bothremydids are known not only from Africa, South America, and Madagascar, but also from North America and Eurasia (Gaffney et al. 2006). The Pangaeic distribution of bothremydids in the Late Cretaceous strongly suggests that the pair of surviving genera on African constitute a relict distribution (Maisey 1993). At least four pelomedusoid lineages are already recorded before the close of the Early Cretaceous (Gaffney et al. 2006).

Laganemys provides one of the closest links to date between the similar age mid Cretaceous faunas (ca. 110 Mya; Aptian–Albian) recovered in the Araripe Basin in Brazil and the Illumeden Basin in Niger, just prior to the advent of deep waters in the central Atlantic Ocean (ca. 100 Mya). In the Araripe Basin, the best known vertebrate fauna comes from concretions in the Romualdo Member of the Santana Formation, which consists of an alternating sequence of lacustrine and fluvial sediments that show occasional marine incursions (Maisey 1993). Numerous specimens of *Araripemys barretoi* have been recovered from the Romualdo Member (Meylan 1996). The diverse Lagertätten from this member includes many soft-bodied invertebrates, although dinosaurs are rare and fragmentary (Naisch et al. 2004).

The rarity of dinosaurs in the Araripe Basin inhibits comparison to the dinosaur and crocodylomorph-rich fauna from the Illumeden Basin of Niger (Taquet 1976; Sereno et al. 1998, 2007; Sereno and Larsson 2009). The comparable strata in the Illumeden Basin are freshwater fluvial sediments of the Elrhaz Formation. Recent finds in Niger include well preserved specimens of the notosuchian crocodylomorph *Araripesuchus wegeneri* (Sereno and Larsson 2009), which is very close in morphology to *Araripesuchus gomesii* (Price 1959) from the Romualdo Member of the Santana Formation. Although differing in only minor ways, these two species of *Araripesuchus* may not be sister taxa; the genus *Araripesuchus* is speciose and broadly distributed across South America, Africa and Madagascar (Sereno and Larson 2009).

Laganemys tenerensis and *Araripemys barretoi*, in contrast, are clearly closest relatives among known pleurodires. Their distribution on each side of the encroaching waters of the mid Atlantic suggests that there was active faunal exchange between these landmasses immediately prior to the Late Cretaceous.

Function

Cervical Reach and Aquatic Feeding

The cervical column in both *Araripemys* and *Laganemys* is approximately 90% of the midline length of the carapace and composed of elongate vertebrae of similar length (Figs. 14.1, 14.2). The marked nuchal embayment at the anterior end of the carapace suggests that this long neck was capable of near vertical excursion.

Considerable lateral mobility with the series is suggested by the form and orientation of the zygapophyseal joints. The fused horizontal postzygapophyseal articular surface is very broad, allowing considerable excursion by the opposing narrower prezygapophyses (Fig. 14.17). The cervical series is preserved along an S-shaped curve, with hyperflexion occurring largely in a horizontal plane between cervical vertebrae 2 and 3 and 6 and 7 (Figs. 14.2, 14.16, 14.18).

Among pleurodires, chelids may provide an extant analog for understanding the function of the proportionately long and flexible cervical series for prey capture in araripemydids. *Chelus fimbriatus*, the matamata or fringed turtle, is a specialized suction feeder that uses fast neck extension and marked bucco-pharyngo-esophageal expansion ("gape and suck") for capture of elusive aquatic prey (Wise et al. 1989; Lemell et al. 2002). *Chelodina longicollis*, the common snake-necked turtle, is less specialized but also uses fast neck extension and bucco-pharyngeal expansion for elusive aquatic prey capture (Van Damme and Aerts 1997). Expansion of the oropharyngeal spaces creates inertial suction that draws prey toward and into the mouth. In both of these chelids, however, the hypoid apparatus is hypertrophied to handle rapid oropharyngeal expansion; there are two sets of ossified ceratobranchials that are enlarged and joined into a rigid basket under the pharynx (Aerts et al. 2001; Lemell et al. 2002). Araripemydids clearly do not have a hypertrophied hyoid apparatus and thus are unlikely to be such specialized aquatic feeders.

Rapid strike neck extension and bucco-pharyngeal expansion, however, also characterizes less specialized, shorter-necked aquatic feeders such as *Chelydra serpentina*, the American snapping turtle (Bramble 1978; Lauder and Prendergast 1992), and *Terrapene nelsoni*, the spotted box turtle (Summers et al. 1998). These cryptodires use less exaggerated bucco-pharyngeal expansion to offset the motion of the head toward the prey, so as not to induce any water flow in the vicinity of the prey. These species, in effect, are underwater "ram-feeders" (Lauder and Prendergast 1992), a feeding function they perform with a pair of ossified rod-shaped ceratobranchials in the floor of the buccal cavity.

These extant analogs, in sum, suggest that araripemydids were long-necked aquatic feeders with rapid strike capability for capture of fish and other elusive prey. Like their extant snake- and shorter-necked analogs, however, they were probably opportunistic feeders with a diet that also included carrion and a range of planktonic and benthic invertebrates (Chessman 1984; Ernst and Barbour 1989). The delicate structure and low profile of their shell and its reduced scutation suggests that araripemydids were fully aquatic and occupied still or slow-moving freshwater habitats similar to those occupied by trionychids, or soft-shelled turtles (Ernst and Barbour 1989).

Limb Proportions

The relative size of the forelimb and hind limb differ markedly between *Laganemys* and *Araripemys*. *Araripemys* exhibits what is likely the primitive and common condition among turtles, in which forelimb bones are slightly shorter than comparable hind limb bones. This comparison is necessarily excludes the humerus and femur, because the length of these bones is not yet known in *Laganemys*.

As shown in reconstruction (Fig. 14.1; Meylan 1996), the radius is approximately 81% of tibial length, and the longest metacarpal (metacarpal 4) is approximately 82% of the longest metatarsal (metatarsal 3) in *Araripemys*. In *Laganemys* the forelimb is considerably shorter than the hind limb. The radius is approximately 59% of tibial length, and the longest metacarpal (metacarpal 4) is approximately 47% of the longest metatarsal (metatarsal 3). In sum, principal forelimb bones in *Laganemys* are 20–30% shorter than in *Araripemys* when measured against comparable hind limb bones (Fig. 14.2).

To determine if these differing limb proportions are due to forelimb reduction or hind limb enlargement, we compare available limb bone lengths to maximum carapace length in these two closely related genera. In *Araripemys* the radius and tibia are approximately 13 and 16% of carapace length, respectively. In *Laganemys* the radius and tibia are approximately 11 and 19% of carapace length, respectively. By this comparison, the radius seems slightly shorter and the tibia slightly longer relative to carapace length in *Laganemys*. Thus it appears from these measurements that both factors, forelimb reduction and hind limb enlargement, may have generated the limb disparity observed in *Laganemys* as compared to *Araripemys*. Enhanced limb disparity, the functional meaning of which is unknown, is regarded here as an autapomorphy for *Laganemys*.

Conclusions

We describe a new long-necked turtle from mid Cretaceous rocks in Niger, *Laganemys tenerensis*, which is closely related to a turtle of similar age from the Araripe Basin in Brazil, *Araripemys barretoi*. These genera provide additional evidence for faunal exchange between South America and Africa in the mid Cretaceous (ca. 110 Mya) prior to the advent of deep waters in the central Atlantic Ocean (Maisey 1993; Sereno and Brusatte 2008).

Their mutual affinity is apparent in the many features they share, not least an extremely long neck and a flat, uniquely textured shell. The position of Araripemydidae among pleurodires remains unresolved. Character data clearly establishes the family as a member of Pelomedusoides. The broad exposure of the prootic on the ventral surface of the braincase in both *Laganemys* and *Araripemys* is one the more convincing plesiomorphies shared with pelomedusids. Podocnemidoid pleurodires, in contrast, cover this bone with others.

Outstanding features of *Laganemys* compared to *Araripemys* involve the elongate skull and the relatively short forelimb. Araripemydids likely lived in slow-moving fluvial and lacustrine habitats as opportunistic feeders capable of fast strike pursuit of elusive prey.

Acknowledgments We would like to thank C. Abraczinskas for executing Figs. 14.2, 14.3, 14.4, 14.11 and 14.24 and for her assistance in layout and formatting of the other figures, R. Masek of the Fossil Lab at the University of Chicago for his extraordinary preparation of the specimen, E. S. Gaffney and F. de Broin de Lapparent for access to specimens in their care and discussions on fossil turtles, the personnel of the High-Resolution X-ray Computed Tomography Facility at The University of Texas at Austin for CT scans of the skull, the field crew of the 2000 Expedition to Niger for discovery of the specimen, and A. Maga and O. Ide of the Institut de Recherche en Sciences Humaines, University of Niamey, Niger, for support and permission for field work. This research was supported by the Biological Sciences Collegiate Division at the University of Chicago and the Association for Women in Science (to SJE) and by the Packard Foundation, the Whitten-Newman Foundation, and the Island Fund of the New York Community Trust (to PCS). The manuscript was reviewed by M. P. J. Ryan, E. S. Gaffney, and T. Konishi.

Appendix

Character scores used in this analysis for *Laganemys tenerensis* gen. et sp. nov. and *Araripemys barretoi*.

(A) Character scores for *Laganemys tenerensis* gen. et sp. nov. for 175 characters in the analysis of Gaffney et al. (2006), all scored from the holotypic skeleton (MNN GAD28).

111100001000121010100000000011101000000033000??
1?10130000201011111111001100300110111111?00?0110
00001100000?13?1102110001000001111210???1???1142
1?022111212111?2?2011110001?10120?5

(B) Character states for *Araripemys barretoi* altered from those given in Gaffney et al. (2006).
Character 30: state 0 changed to state 1.
Character 40: state 0 to state 3.
Character 147: state 3 to ?.

References

Aerts, P., Van Damme, J., & Herrel, A. (2001). Intrinsic mechanics and control of fast cranio-cervical movements in aquatic feeding turtles. *American Zoologist, 41*, 1299–1310.

Baur, A. M. (1993). Africa–South American relationships: A perspective from the Reptilia. In P. Goldblatt (Ed.), *Biological relationships between Africa and South America* (pp. 244–288). New Haven: Yale University Press.

Bickham, J. W., Parham, J. F., Philippen, H. D., & Rhodin, A. G. J. (2007). Turtle taxonomy: Methodology, recommendations, and guidelines. *Chelonian Research Monographs, 4*, 73–84.

Bonnaterre, J. P. (1789). *Tableau Encyclopédique et Méthodique des Trois Règnes de la Nature*. Paris: Panckoucke.

Bramble, D. M. (1978). Functional analysis of underwater feeding in the snapping turtle. *American Zoologist, 18*, 230–261.

Chessman, B. C. (1984). Food of the snake-necked turtle, *Chelodina longicollis* (Shaw) (Testudines: Chelidae) in the Murray Valley. *Australian Wildlife Research, 11*, 573–578.

Cope, E. D. (1865). Third contribution to the herpetology of tropical America. *Proceedings of the Academy of Natural Sciences of Philadelphia, 17*, 185–198.

Cope, E. D. (1868). On the origin of genera. *Proceedings of the Academy of Natural Sciences of Philadelphia, 20*, 242–300.

de Broin, F. (1980). Les tortues de Gadoufaoua (Aptien du Niger); aperçu sur la Paléobiogéographie des Pelomedusidae (Pleurodira). *Mémoires de la Société Géologique de France, 139*, 39–46.

de Broin, F. (1988). Les tortues et le Gondwana. Examen des rapports entre le fractionnement du Gondwana au Crétacé et la dispersion géographique des tortues pleurodires á partir du Crétacé. *Studia Geologica Salmanticensia. Studia Palaeocheloniologica, 2*, 103–142.

de la Fuente, M., & de Lapparent de Broin, F. (1997). An Araripemys-like decorated pleurodire turtle in the Paleocene of northwestern Argentine. *Geobios*, *30*, 235–242.

de Queiroz, K., & Gauthier, J. (1990). Phylogeny as a central principle in taxonomy: Phylogenetic definitions of taxon names. *Systematic Zoology, 39*, 307–322.

de Queiroz, K., & Gauthier, J. (1992). Phylogenetic taxonomy. *Annual Review of Ecology and Systematics, 23*, 449–480.

Ernst, C. H., & Barbour, R. W. (1989). *Turtles of the world*. Washington, DC: Smithsonian Institution Press.

Fielding, S., Martill, D. M., & Naish, D. (2005). Solnhofen style soft-tissue preservation in a new species of turtle from the Crato Formation (Early Cretaceous, Aptian) of north-east Brazil. *Palaeontology, 48*, 1301–1310.

Gaffney, E. S. (1972). An illustrated glossary of turtle skull nomenclature. *American Museum Novitates, 2486*, 1–33.

Gaffney, E. S. (1975). A phylogeny and classification of the higher categories of turtles. *Bulletin of the American Museum of Natural History, 155*, 389–436.

Gaffney, E. S. (1979). Comparative cranial morphology of recent and fossil turtles. *Bulletin of the American Museum of Natural History, 164*, 1–376.

Gaffney, E. S. (1984). Historical analysis of theories of chelonian relationship. *Systematic Biology, 33*, 283–301.

Gaffney, E. S. (1990). The comparative osteology of the Triassic turtle *Proganochelys*. *Bulletin of the American Museum of Natural History, 194*, 1–263.

Gaffney, E. S., Hutchinson, J. H., Jenkins, F. A., Jr., & Meeker, L. J. (1987). Modern turtle origins: The oldest known cryptodire. *Science, 237*, 289–291.

Gaffney, E. S., Tong, H., & Meylan, P. A. (2006). Evolution of the side-necked turtles: The families Bothremydidae, Euraxemydidae, and Araripemydidae. *Bulletin of the American Museum of Natural History, 300*, 1–698.

Gaffney E.S., & Meylan, P.A. (1988). A phylogeny of turtles. In M. J. Benton (Ed.) *The Phylogeny and Classification of the Tetrapods: Amphibians, Reptiles, Birds* (pp. 157–219). Oxford: Clarendon Press.

Gray, J. E. (1825). A synopsis of the genera of reptiles and amphibia, with a description of some new species. *Annals of Philosophy, 10*, 193–217.

Hennig W. (1966). *Phylogenetic Systematics*. Urbana: University of Illinois Press, pp. 263.

Hirayama, R. (1991). *Phylogenetic relationship of Araripemys* (*family Araripemydidae*; *Pleuroria*; *Testudinata*). Abstracts of the 140th regular meeting of the Palaeontological Society of Japan, June 22, 23, 1991, Chiba.

ICZN. (Ed.) (1999). *International Code of Zoological Nomenclature*. London: The International Trust for Zoological Nomenclature.

Joyce, W. G. (2007). Phylogenetic relationships of Mesozoic turtles. *Bulletin of the Peabody Museum of Natural History, 48*, 3–102.

Joyce, W. G., Parham, J. F., & Gauthier, J. A. (2004). Developing a protocol for the conversion of rank-based taxon named to phylogenetically defined clade names, as exemplified by turtles. *Journal of Paleontology, 78*, 989–1013.

Lemell, P., Lemell, C., Snelderwaard, P., Gumpenberger, M., Wocheslander, R., & Weisgram, J. (2002). Feeding patterns of *Chelus fimbriatus* (Pleurodira: Chelidae). *Journal of Experimental Biology, 205*, 1495–1506.

Lauder, G. V., & Prendergast, T. (1992). Kinematics of aquatic prey capture in the snapping turtle *Chelydra serpentina*. *Journal of Experimental Biology, 164*, 55–78.

Linnaeus, C. (1758). *Systema Naturae per Raegna Tria Naturae*. *Volume 1*. *Regnum Animale* (10th ed.) Photographic facsimile. London: Trustees, British Museum (Natural History).

Maisey, J. G. (1991). *Santana fossils: An illustrated Atlas*. Neptune, NJ: Tropical Fish Hobbyist Publications.

Maisey, J. G. (1993). Tectonics, the Santana Lagerstätten, and the implications for late Gondwanan biogeography. In P. Goldblatt (Ed.), *Biological relationships between Africa and South America* (pp. 435–454). New Haven: Yale University Press.

Meylan, P. A. (1996). Skeletal morphology and relationships of the Early Cretaceous side-necked turtle, *Araripemys barretoi* (Testudines: Pelomedusoides: Araripemydidae), from the Santana Formation of Brazil. *Journal of Vertebrate Paleontology, 16*, 20–33.

Meylan, P. A., & Gaffney, E. S. (1991). Araripemys Price, 1973. In J. G. Maisey (Ed.), *Santana fossils: An illustrated Atlas* (pp. 326–334). Neptune, NJ: Tropical Fish Hobbyist Publications.

Naish, D., Martill, D. M., & Frey, E. (2004). Ecology, systematics and biogeographical relationships of dinosaurs, including a new theropod, from the Santana Formation (?Albian, Early Cretaceous) of Brazil. *Historical Biology, 16*, 57–70.

Noonan, B. P. (2000). Does the phylogeny of pelomedusoid turtles reflect vicariance due to continental drift? *Journal of Biogeography, 27*, 1245–1249.

Price, L. I. (1959). Sobre um cocodrilideo Notosuquio do Cretácico Brasileiro. *Departamento Nacional da Produção Mineral, Divisão de Geología e Mineralogía, Río de Janeiro, 188*, 7–55.

Price, L. I. (1973). Quelônio amphichelydia do Cretáceo inferior do nordeste do Brasil. *Brazileira de Geociências, 3*, 84–96.

Pritchard, P. C. H. (1979). *Encyclopedia of turtles*. Neptune, NJ: Tropical Fish Hobbyist Publications.

Romer, A. S. (1956). *Osteology of the Reptilia*. Chicago: University of Chicago Press.

Rueda, E. A. C., & Gaffney, E. S. (2005). *Notoemys zapatocaensis*, a new side-necked turtle (Pleurodira: Platychelyidae) from the Early Cretaceous of Colombia. *American Museum Novitates, 3470*, 1–19.

Schneider, J. G. (1783). *Allgemeine Naturgeschichte der Schildkröten, nebst einem Systematischen Verseichnisse der einzelnen Arten und zwey Kupfern*. Leipzig: Johan Gotfried Müllersche Buchhandlung.

Schweigger, A. F. (1812). Prodromus monographiae Cheloniorum, Pt. 1. *Königsberger Achiv für Naturwissenschaft und Mathematik, 1812*, 271–458.

Sereno, P. C. (2005). The logical basis of phylogenetic taxonomy. *Systematic Biology, 54*, 595–619.

Sereno, P. C. (2007). Logical basis for morphological characters in phylogenetics. *Cladistics, 23*, 565–587.

Sereno, P. C., & Brusatte, S. L. (2008). Basal abelisaurid and carcharodontosaurid theropods from the Lower Cretaceous Elrhaz Formation of Niger. *Acta Palaeontologica Polonica, 53*, 15–46.

Sereno, P. C., & ElShafie, S. (2009). The unusual South American pelomedusoid turtle, *Araripemys*, discovered in Africa. *Journal of Vertebrate Paleontology, 11*(Suppl), 180A.

Sereno, P. C., & Larsson, H. C. E. (2009). Cretaceous Crocodyliforms from the Sahara. *ZooKeys, 28*, 1–143.

Sereno, P. C., Beck, A. L., Dutheil, D. B., Gado, B., Larsson, H. C. E., & Lyon, G. H. (1998). A long-snouted predatory dinosaur from Africa and the evolution of spinosaurids. *Science, 282*, 1298–1302.

Sereno, P. C., Wilson, J. A., & Conrad, J. L. (2004). New dinosaurs link southern landmasses in the Mid-Cretaceous. *Proceedings of the Royal Society of London B, 271*, 1325–1330.

Summers, A. P., Darouian, K. F., Richmond, A. M., & Brainerd, E. L. (1998). Kinematics of aquatic and terrestrial prey capture in *Terrapene carolina*, with implications for the evolution of feeding in cryptodire turtles. *Journal of Experimental Zoology Part A, Comparative Experimental Biology, 281*, 280–287.

Taquet, P. (1976). Géologie et paléontologie du gisement de Gadoufaoua (Aptian du Niger). *Cahiers de Paléontologie, 1976*, 1–191.

Van Damme, J., & Aerts, P. (1997). Kinematics and functional morphology of aquatic feeding in Australian snake-necked turtles (Pleurodira; *Chelodina*). *Journal of Morphology, 233*, 113–125.

Wilson, J. A. (2006). Anatomical nomenclature of fossil vertebrates: Standardized terms or 'lingua franca'? *Journal of Vertebrate Paleontology, 26*, 511–518.

Wise, S. C., Formanowicz, D. R., Jr., & Brodie, E. D., Jr. (1989). Matamata turtles ambush but do not herd prey. *Journal of Herpetology, 23*, 297–299.